Unclassified **NEA/CSNI/R(2010)6**

Organisation de Coopération et de Développement Économiques
Organisation for Economic Co-operation and Development **15-Nov-2010**

English text only

NUCLEAR ENERGY AGENCY
COMMITTEE ON THE SAFETY OF NUCLEAR INSTALLATIONS

Benchmark Calculations on Halden IFA-650 LOCA Test Results

JT03292496

NEA/CSNI/R(2010)6
Unclassified

English text only

ORGANISATION FOR ECONOMIC CO-OPERATION AND DEVELOPMENT

The OECD is a unique forum where the governments of 33 democracies work together to address the economic, social and environmental challenges of globalisation. The OECD is also at the forefront of efforts to understand and to help governments respond to new developments and concerns, such as corporate governance, the information economy and the challenges of an ageing population. The Organisation provides a setting where governments can compare policy experiences, seek answers to common problems, identify good practice and work to co-ordinate domestic and international policies.

The OECD member countries are: Australia, Austria, Belgium, Canada, Chile, the Czech Republic, Denmark, Finland, France, Germany, Greece, Hungary, Iceland, Ireland, Israel, Italy, Japan, Korea, Luxembourg, Mexico, the Netherlands, New Zealand, Norway, Poland, Portugal, the Slovak Republic, Slovenia, Spain, Sweden, Switzerland, Turkey, the United Kingdom and the United States. The European Commission takes part in the work of the OECD.

OECD Publishing disseminates widely the results of the Organisation's statistics gathering and research on economic, social and environmental issues, as well as the conventions, guidelines and standards agreed by its members.

NUCLEAR ENERGY AGENCY

The OECD Nuclear Energy Agency (NEA) was established on 1st February 1958 under the name of the OEEC European Nuclear Energy Agency. It received its present designation on 20th April 1972, when Japan became its first non-European full member. NEA membership today consists of 28 OECD member countries: Australia, Austria, Belgium, Canada, the Czech Republic, Denmark, Finland, France, Germany, Greece, Hungary, Iceland, Ireland, Italy, Japan, Korea, Luxembourg, Mexico, the Netherlands, Norway, Portugal, the Slovak Republic, Spain, Sweden, Switzerland, Turkey, the United Kingdom and the United States. The European Commission also takes part in the work of the Agency.

The mission of the NEA is:

– to assist its member countries in maintaining and further developing, through international co-operation, the scientific, technological and legal bases required for a safe, environmentally friendly and economical use of nuclear energy for peaceful purposes, as well as

– to provide authoritative assessments and to forge common understandings on key issues, as input to government decisions on nuclear energy policy and to broader OECD policy analyses in areas such as energy and sustainable development.

Specific areas of competence of the NEA include safety and regulation of nuclear activities, radioactive waste management, radiological protection, nuclear science, economic and technical analyses of the nuclear fuel cycle, nuclear law and liability, and public information.

The NEA Data Bank provides nuclear data and computer program services for participating countries. In these and related tasks, the NEA works in close collaboration with the International Atomic Energy Agency in Vienna, with which it has a Co-operation Agreement, as well as with other international organisations in the nuclear field.

COMMITTEE ON THE SAFETY OF NUCLEAR INSTALLATIONS

Within the OECD framework, the NEA Committee on the Safety of Nuclear Installations (CSNI) is an international committee made of senior scientists and engineers, with broad responsibilities for safety technology and research programmes, as well as representatives from regulatory authorities. It was set up in 1973 to develop and co-ordinate the activities of the NEA concerning the technical aspects of the design, construction and operation of nuclear installations insofar as they affect the safety of such installations.

The committee's purpose is to foster international co-operation in nuclear safety amongst the NEA member countries. The CSNI's main tasks are to exchange technical information and to promote collaboration between research, development, engineering and regulatory organisations; to review operating experience and the state of knowledge on selected topics of nuclear safety technology and safety assessment; to initiate and conduct programmes to overcome discrepancies, develop improvements and research consensus on technical issues; and to promote the co-ordination of work that serves to maintain competence in nuclear safety matters, including the establishment of joint undertakings.

The clear priority of the committee is on the safety of nuclear installations and the design and construction of new reactors and installations. For advanced reactor designs the committee provides a forum for improving safety related knowledge and a vehicle for joint research.

In implementing its programme, the CSNI establishes co-operate mechanisms with the NEA's Committee on Nuclear Regulatory Activities (CNRA) which is responsible for the programme of the Agency concerning the regulation, licensing and inspection of nuclear installations with regard to safety. It also co-operates with the other NEA's Standing Committees as well as with key international organizations (e.g., the IAEA) on matters of common interest.

FOREWORD

The assessment of the consequences of a loss-of-coolant accident (LOCA) is to a large extent based on calculations carried out with codes especially developed for addressing the phenomena occurring during the transient. Such codes must also show an appropriate performance with respect to high burnup phenomena influencing LOCA fuel behaviour.

The NEA Working Group on Fuel Safety (WGFS) is tasked with advancing the understanding of fuel safety issues by assessing the technical basis for current safety criteria and their applicability to high burnup and to new fuel designs and materials. The group aims at facilitating international convergence in this area, including the review of experimental approaches as well as the interpretation and use of experimental data relevant for safety.

As a contribution to this task, WGFS conducted a code benchmark based on the Halden LOCA test series. Emphasis was on the codes' ability to predict or reproduce the dynamic behaviour of the experimental system and in particular the thermal and mechanical response of fuel and cladding.

This report provides a summary of the results of this task.

ACKNOWLEDGMENTS

Gratitude is expressed to the OECD Halden Reactor Project (HRP) for providing the benchmark data and in particular to staff seconded to the OECD HRP who followed up the Halden LOCA test series and the WGFS benchmarks. Special thanks therefore go to Mirkka Ek (Fortum Nuclear Services Ltd), Laura Kekkonen (VTT), and Radomír Jošek (NRI) for their work and contributions incorporated in this report. Thanks also go to Wolfgang Wiesenack (HRP) for combining all the contributions and drafting the report.

The following WGFS members and experts from the industry performed calculations and provided valuable input to various chapters of the report:

Yacine Aounallah (PSI, Switzerland)

Claude Grandjean (IRSN, France)

Joachim Herb (GRS, Germany)

Seppo Kelppe (VTT, Finland)

Georg Lerchl (GRS, Germany)

Tetsuo Nakajima (JNES, Japan)

Heinz-Günther Sonnenburg (GRS, Germany)

Gerold Spykman (TÜV Nord, Germany)

J.-O. Stengård (VTT, Finland)

Christine Struzik (CEA, France)

Klaus Trambauer (GRS, Germany)

Hannu Wallin (PSI, Switzerland)

TABLE OF CONTENTS

List of Figures

List of Tables

List of abbreviations

CEA	Commissariat à l'Énergie Atomique
ECCS	Emergency core cooling system
ECR	Equivalent cladding reacted
EPRI	Electric Power Research Institute
GRS	Gesellschaft für Anlagen- und Reaktorsicherheit
HRP	OECD Halden Reactor Project
IFA	Instrumented fuel assembly
IFE	Institutt for energiteknikk (Norway)
IRSN	Institut de Radioprotection et de Sûreté Nucléaire
JNES	Japan Nuclear Energy Safety Organization
LHGR	Linear heat generation rate
LOCA	Loss-of-coolant accident
LWR	Light water reactor
NEA	Nuclear Energy Agency
NRI	Nuclear Research Institute (Czech Republic)
PBF	Power burst facility
PCT	Peak clad temperature
PIE	Post irradiation examination
PSI	Paul Scherrer Institut (Switzerland)
PWR	Pressurised water reactor
SPND	Self-powered neutron detector
TC	Thermocouple
TCCn	Denomination of cladding thermocouple in Halden LOCA tests
TCHn	Denomination of heater thermocouple in Halden LOCA tests
TÜV	Technischer Überwachungsverein
USNRC	United States Nuclear Regulatory Commission
VTT	Valtion Teknillinen Tutkimuskeskus / Technical Research Centre of Finland
WGFS	Working group on fuel safety

EXECUTIVE SUMMARY

The assessment of the consequences of a loss-of-coolant accident (LOCA) is to a large extent based on calculations carried out with codes especially developed for addressing the phenomena occurring during the transient. Such codes must also show an appropriate performance with respect to high burnup phenomena influencing LOCA fuel behaviour.

The Halden LOCA series, using high burnup fuel segments, contains test cases well suited for checking the ability of LOCA analysis codes to predict or reproduce the measurements and to provide clues as to where the codes need to be improved. The NEA Working Group on Fuel Safety, WGFS, therefore conducted a code benchmark based on the Halden LOCA test series. Emphasis was on the codes' ability to predict or reproduce the thermal and mechanical response of fuel and cladding.

Before starting the benchmark, participants were given the opportunity to tune their codes to the experimental system applied in the Halden LOCA tests. To this end, the data from the two commissioning runs were made available.

The benchmark itself, which was conducted in two parts, comprised the Halden experiments IFA-650.3, 650.4 and 650.5 with fuel provided by Framatome ANP. The segments had been irradiated in a commercial PWR to very high burnup, 82, 92 and 83 MWd/kgU, respectively. They were subjected to the LOCA transient in a single rod configuration using a pressure flask connected to a water loop and blow-down system. A low level of nuclear power generation in the fuel rod simulated decay heat, whereas an electrical heater surrounding the rod simulated the heat from neighbour rods. Regarding experimental conditions, the experiments differed mainly in the target peak cladding temperature (PCT). These were 800 °C for the first two tests and 1150 °C for IFA-650.5.

The benchmarks concentrated on the thermal and mechanical response of the fuel and cladding, including the effect of fuel relocation as one of the primary objectives of the Halden test series. The other objective, namely to investigate the extent of "secondary transient hydriding" on the inner side of the cladding above and below the burst region, was not addressed by the codes since the experiments were not conducted in the high temperature oxidation phase of the transient.

The first benchmark of the test IFA 650.3 was implemented as three rounds of calculations starting with a blind pre-test calculation. The results differed amongst the codes and also between the calculation rounds.

In the first round, the codes underpredicted the time to burst. This was largely fixed in the second round of calculation where the agreement between predicted and measured burst time was good. In the third round of calculation using unified thermo-hydraulic boundary conditions, three codes overpredicted the time to burst.

The codes were able to render the dynamics of the fairly complicated experimental system in a satisfactory way. The calculated heater temperatures showed a larger spread and deviation from the measured value,

possibly due to sensitivity of the calculations to emissivity values, which was also observed when the codes were calibrated to the system with the commissioning runs.

Strain profiles at burst showed severe over-prediction of strain in all three cases in all codes. This is understandable since the experiment did not develop as foreseen and failed at a weak spot introduced by thermocouple welding. However, the spread of calculated ballooning strains even when uniform boundary conditions were applied indicates that the associated modelling can still be improved.

The second benchmark using data from the Halden LOCA series IFA 650.4 and IFA 650.5 was completed by four codes: Athlet-CD (GRS), Fraptran-Genflo (VTT), Icare-Cathare (IRSN), and Meteor (CEA). These codes participated in the first phase as well and contained modifications and improvements to be able to render the Halden experiments in a better way.

On average, the codes agreed reasonably with the experimental results.

Regarding rod pressure, the effect of ballooning causing the pressure to decrease was well calculated by the codes, implying that also the ballooning strain is calculated with a similar degree of agreement with the measured maximum strain of about 62%. Also regarding time to failure at measured 336s, the results were within an acceptable range of deviation (308 – 340 s).

The most critical calculation is the cladding temperature since it is directly linked to the safety criterion limit of peak clad temperature and has a strong influence on cladding oxidation which is limited by the ECR safety criterion. The peak temperature as measured at the upper thermocouple position in IFA-650.4 was reproduced well by all codes and agreed with the measurement within 35 degrees C. The codes were conservative in that the results were slightly higher than measured.

As an improvement, the codes introduced the effect of fuel relocation on cladding temperature. The principal effect seems to be well described. However, improvements regarding details of the temperature response to fuel relocation should still be sought since the codes will be used to evaluate a potentially critical part of a safety assessment.

Fuel relocation as seen in IFA-650.4 is not a singular occurrence – as demonstrated with Halden LOCA test 650.9 carried out with 650.4 sibling fuel on April 17, 2009. The observations underline the importance that codes for LOCA analysis should be improved to model the relocation phenomenon and calculate the consequences on local cladding oxidation and embrittlement.

1. INTRODUCTION AND BACKGROUND

The assessment of the consequences of a loss-of-coolant accident (LOCA) is to a large extent based on calculations carried out with codes especially developed for addressing the phenomena occurring during the transient. Since the time of the first LOCA experiments, which were largely conducted with fresh fuel, changes in fuel design, the introduction of new cladding materials and in particular the move to high burnup have not only generated a need to re-examine the LOCA safety criteria and to verify their continued validity, but also to confirm that codes show an appropriate performance especially with respect to high burnup phenomena influencing LOCA fuel behaviour.

As part of international efforts, the OECD Halden Reactor Project program implemented a test series to address particular LOCA issues. Based on recommendations of a group of experts from the USNRC, EPRI, EDF, FRAMATOME-ANP and GNF, the primary objective of the experiments were defined as

1. Measure the extent of fuel (fragment) relocation into the ballooned region and evaluate its possible effect on cladding temperature and oxidation.

2. Investigate the extent (if any) of "secondary transient hydriding" on the inner side of the cladding above and below the burst region.

The Halden LOCA series, using high burnup fuel segments, contains test cases well suited for checking the ability of LOCA analysis codes to predict or reproduce the measurements and to provide clues as to where the codes need to be improved. The NEA Working Group on Fuel Safety, WGFS, therefore decided to conduct a code benchmark based on the Halden LOCA test series. Emphasis was on the codes' ability to predict or reproduce the thermal and mechanical response of fuel and cladding.

Before starting the benchmark, participants were given the opportunity to tune their codes to the experimental system applied in the Halden LOCA tests. To this end, the data from the two commissioning runs were made available. The first of these runs went through several blow-downs and heat-ups and reached peak clad temperatures of more than 1000 C. In the second run, where the rod was sufficiently pre-pressurised, ballooning and burst was obtained.

The first benchmark consisted of three rounds of code calculations related to IFA-650.3:

1. Pre-test calculations: Participants were provided with information regarding the setup of the Halden LOCA test facility, data from the commissioning runs, and information about the test pin and power conditions to be applied in the execution of the test.

2. Post-test calculations I: In addition to the information from the first round, participants were provided with the in-pile results from the test.

3. Post-test calculations II, unified thermal-hydraulic boundary conditions: Calculations were repeated using a cladding temperature distribution calculated with ATHLET-CD at GRS.

Since the test, when executed, did not produce the expected ballooning and fuel relocation, it was decided to continue with a second benchmark using tests 650.4 and 650.5, this time as post-test calculations.

The fourth test of the series, IFA-650.4 conducted in April 2006, caused particular attention in the international nuclear community. The fuel used in the experiment had a high burnup, 92 MWd/kgU, and a low pre-test hydrogen content of about 50 ppm. The cladding burst at about 790 °C caused a marked temperature increase at the lower end of the segment and a decrease at the upper end, indicating that fuel relocation had occurred. Subsequent gamma scanning showed that approximately 19 cm (40%) of the fuel stack were missing from the upper part of the rod. PIE at the IFE-Kjeller hot cells corroborated this evidence of substantial fuel relocation.

This report presents the results of the codes which participated in the various benchmarks. The two main parts, on benchmark I and II, each start with a brief description of the most important experimental data. Then, the code calculation results follow.

2. GENERAL DESCRIPTION OF THE TEST SET-UP

The fuels for IFA-650.3, 650.4 and 650.5 were provided by Framatome ANP. The segments had been irradiated in a commercial PWR to very high burnup, 82, 92 and 83 MWd/kgU, respectively. Regarding experimental conditions, the experiments differed mainly in the target peak cladding temperature (PCT). These were 800 °C for the first two tests and 1150 °C for IFA-650.5.

2.1 Rig structure and instrumentation

A single fuel rod is inserted into a pressure flask connected to a water loop (Fig. 1). A low level of nuclear power generation in the fuel rod is used to simulate decay heat, whereas the electrical heater surrounding the rod is simulating the heat from neighbour rods.

The rod instrumentation consists of two cladding thermocouples (TC) at the upper part of the rod, one cladding TC at the lower part, two heater thermocouples (at two different axial elevations), a cladding extensometer and a rod pressure sensor. The denomination of the thermocouples is TCCn for the cladding and TCHn for the heater.

The rig contains coolant thermocouples (two at rig inlet and two at outlet), three axially distributed vanadium neutron detectors to measure the axial power distribution, and two fast response cobalt SPNDs to monitor rapid flux and power changes.

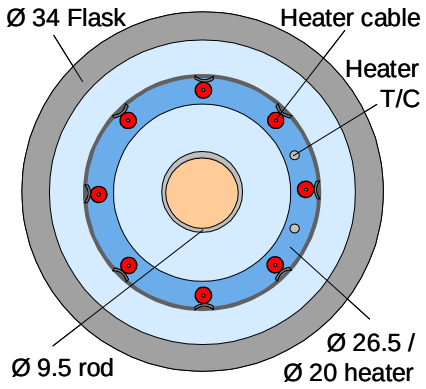

Fig. 1 - Cross section of fuel pin, heater and pressure tube used in HRP LOCA studies

The instrumentation differs slightly in individual cases from this general layout, especially regarding cladding thermocouples. This is indicated in the respective detailed descriptions.

2.2 Test execution principles

Before the test execution, the reactor is operated for 7-8 hours at about 15 MW (fuel average linear heat rate about 85 W/cm). After power calibration, the LOCA test is performed at a reactor power of 4.0 MW and a low rod power (10-30 W/cm depending on target PCT). The axial power profile is nearly symmetric with an axial peak to average power factor of ≈1.05.

The test is initiated by opening the blow-down line at the bottom of the rig. Then, the changes like heat-up, ballooning and burst go their course according to the dynamic behaviour of the system without interference by experimenters apart from injecting small amounts of water/steam during the high temperature phase after burst. This is done in order to maintain a sufficient amount of steam for the cladding oxidation.

The termination criteria are:

- reaching the 17% ECR limit (this was not the case in any of the experiments executed within the Halden LOCA series so far);
- having run the experiment for about 5 minutes after blow-down (a LOCA would normally not last longer than that if the ECCS responds as foreseen);
- detecting signs of secondary degradation after ballooning, e.g. that the fuel rod would break.

The experiments are terminated by switching off the electrical heating and scramming the reactor such that the fission heat generation in the fuel rod ceases. The test rods are allowed to cool down relatively slowly with the reactor. Quenching, although included in the experimental possibilities of the system, is not applied. This is a deliberate choice with the purpose to avoid any disturbances, e.g. vibrations, which might influence a possible fuel relocation that had developed so far during the experiment.

3. BENCHMARK I - TEST EXECUTION AND PRINCIPAL OBSERVATIONS

IFA-650.3, the first test with pre-irradiated fuel in the Halden Project LOCA series, was used for the first benchmark. It was conducted on April 30, 2005.

The experimental arrangements of the test were similar to those tried out in the commissioning tests, as described in section 2.1. The target temperature of about 800 C was achieved and cladding failure occurred. However, as later inspection revealed, the ballooning did not fully develop because of premature cladding failure at a weak spot introduced by cladding surface thermocouple welding.

3.1 Measurements and observations

The measured cladding and heater temperatures and heater power are shown in Fig. 2. The target cladding temperature of 800 ºC was reached; the temperature at the time of burst (≈267 s after blow-down) at TCC1 (lower end) was 775 ºC and about 10 degrees lower at TCC2 and TCC4 (upper end). Gradual cooling occurred when the reactor was scrammed after about 610 s into the transient.

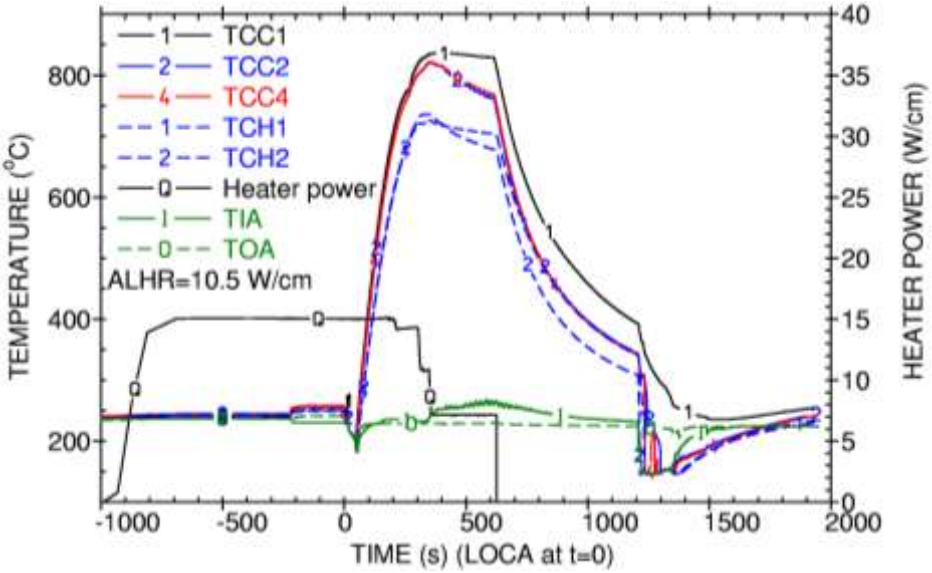

Fig. 2 - Cladding (TCC), heater (TCH), coolant inlet/ outlet (TIA/ TOA) temperatures, and heater power during IFA-650.3

The indications of cladding failure can be seen in Fig. 3. The fast rod pressure drop starts at 267 s. At the same time a response is seen in the elongation signal. The gamma monitor on the blow-down line reacts to the burst about 40 s later. No signs of fuel relocation were seen in the measurements.

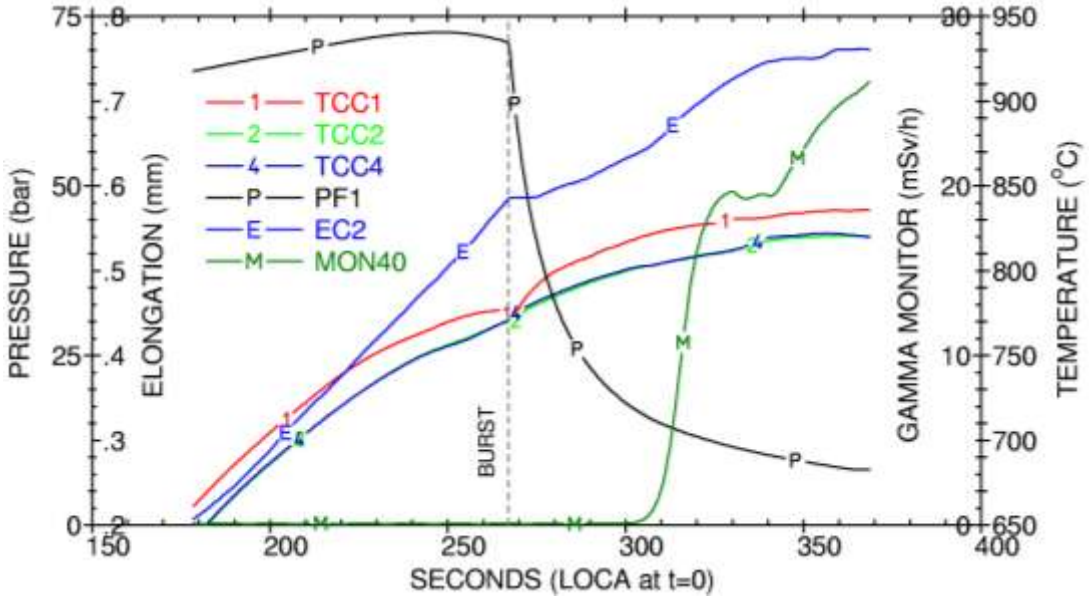

Fig. 3 - Cladding burst indications in IFA-650.3

The pressure maximum was measured at about 250 s after the beginning of the LOCA, i.e. ballooning probably started at this time, ≈20 seconds before failure.

3.2 Post-irradiation examinations

Diameter traces for four orientations are shown in Fig. 4. The diameter increased along the entire rod (maximum about 7%). An incipient local ballooning can be seen at half height where power and temperature are expected to be highest. Another local ballooning developed at the lower end where the welding of the thermocouple caused a hot spot and slight thinning of the cladding. Failure eventually occurred at this location.

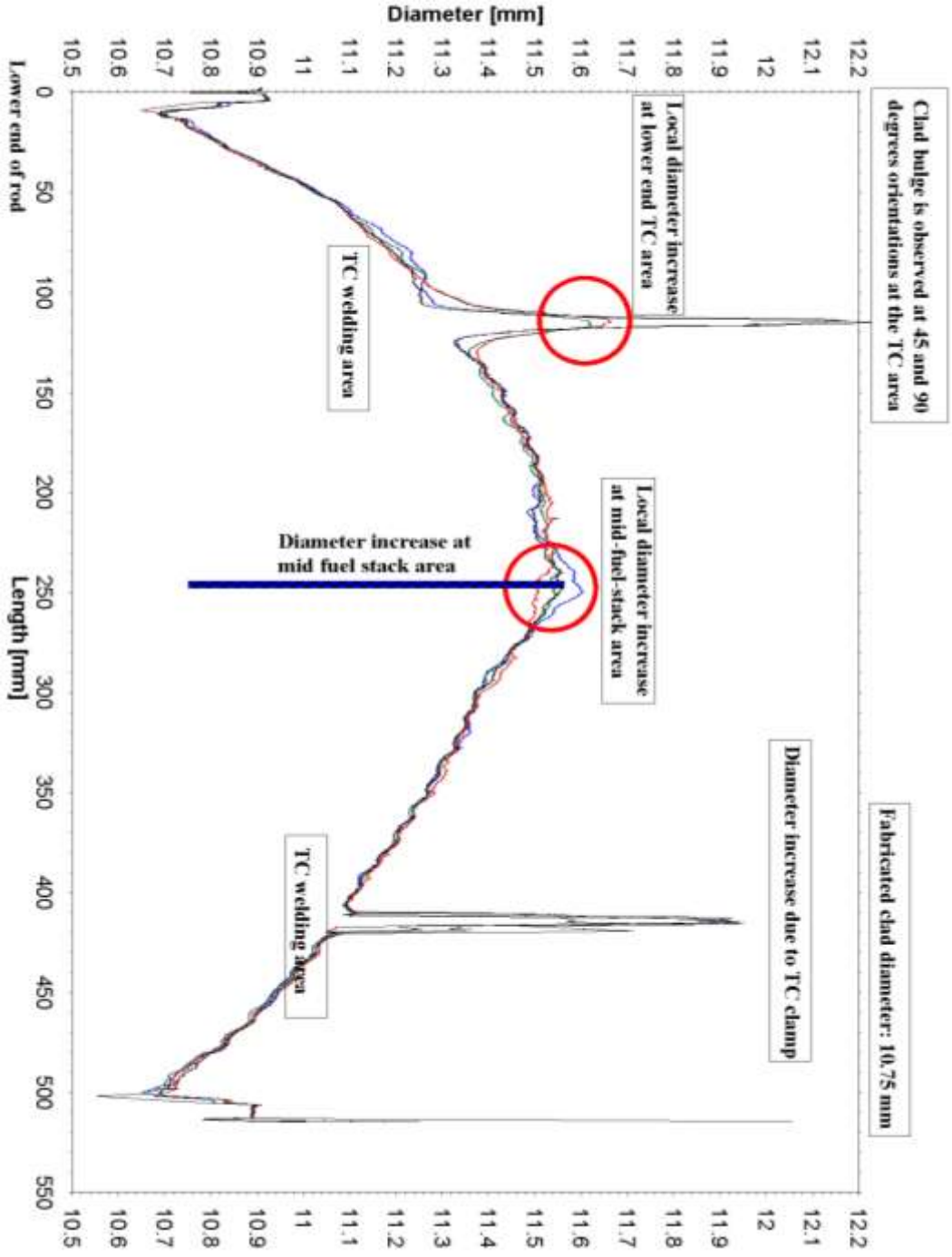

Fig. 4 - Diameter of IFA-650.3 after LOCA test in the Halden reactor. Orientations 0, 45, 90 and 135 degrees

4. BLIND CALCULATIONS – COMPARISON OF RESULTS

Nine codes participated in the first benchmark. The participation in the individual rounds of calculations is summarized in "Appendix II – Benchmark participation". Summary figures were made to compare the results of the participating codes. For better comparison, the times were shifted such that the calculated start of heat-up after blow-down occurred at the same time as measured. This adjustment was made to all figures that are denoted as "(adjusted)".

4.1 Pressure behaviour

The rig pressure behaviour during blow-down was fairly well predicted by most codes, see Fig. 5. The actually measured blow-down time was somewhat affected by an unintentional closing of the second blow-down valve just 2 seconds after the start. The valve was reopened after 10 s. This did not affect the test, but the total time to complete blow-down was increased by ~10 s which should be kept in mind when comparing results and measurements.

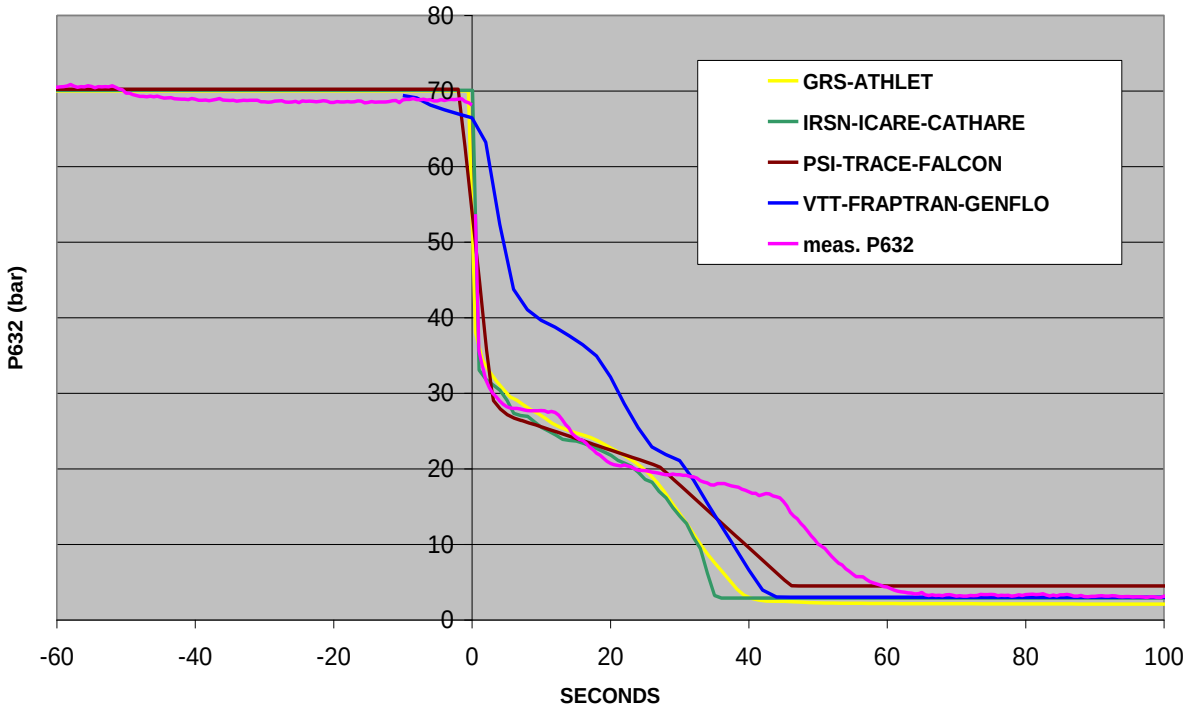

Fig. 5 – Rig pressure drop at blow-down (adjusted)

4.2 Ballooning and failure

All codes predicted ballooning and failure to occur slightly earlier than measured, see Fig. 6 and Tab. 1.

Tab. 1 - Predicted time to burst for blind calculations

Code	Burst time (s)
GRS-ATHLET	NA
GRS-ATHLET-CD	220
GRS-ATHLET-TESPA	203
IRSN-ICARE-CATHARE	189
JNES-TRAC_PF1	NA
PSI-TRACE-FALCON	227
TÜV-TRANSURANUS (GRS-ATHLET)	237
VTT-FRAPTRAN-GENFLO	221 & 210
CEA-METEOR	-
MEASURED	267

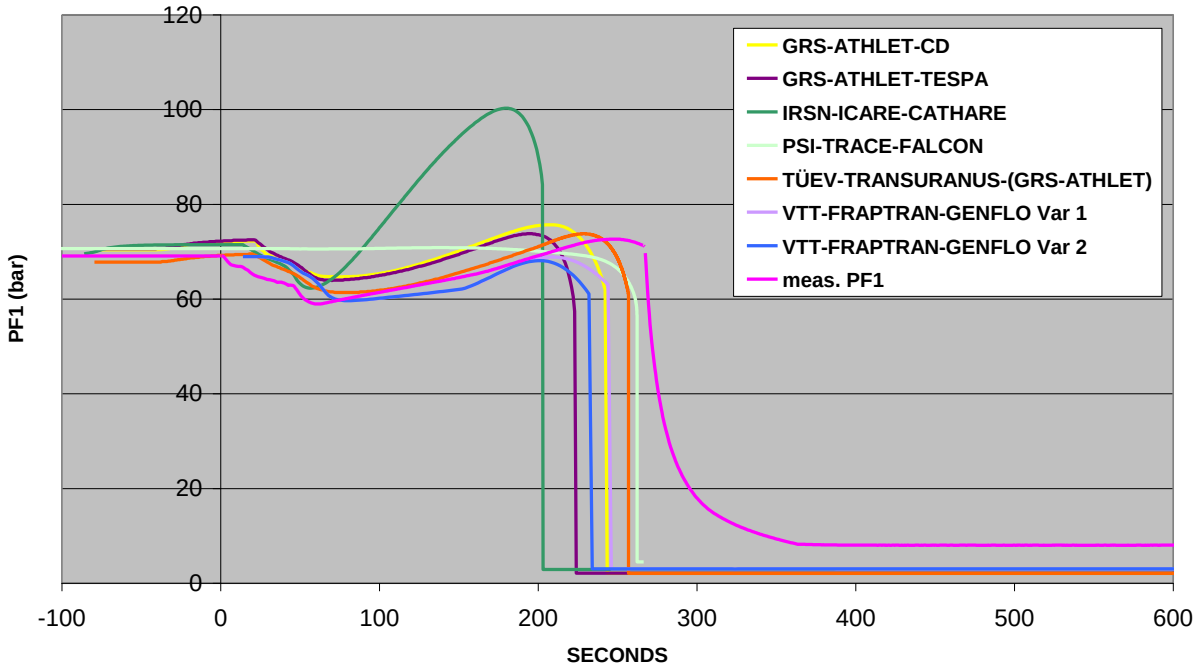

Fig. 6 – Rod pressure reading (adjusted)

4.3 Temperatures

No code could predict the slightly bottom heavy cladding temperature profile at burst time (Fig. 7). The reason for the higher temperatures measured at the bottom is not really known. One possible explanation is water condensing in the outlet line and dropping back during the heat-up. This could provide some local cooling to the upper part of the rod. In general, cladding temperatures were quite well predicted.

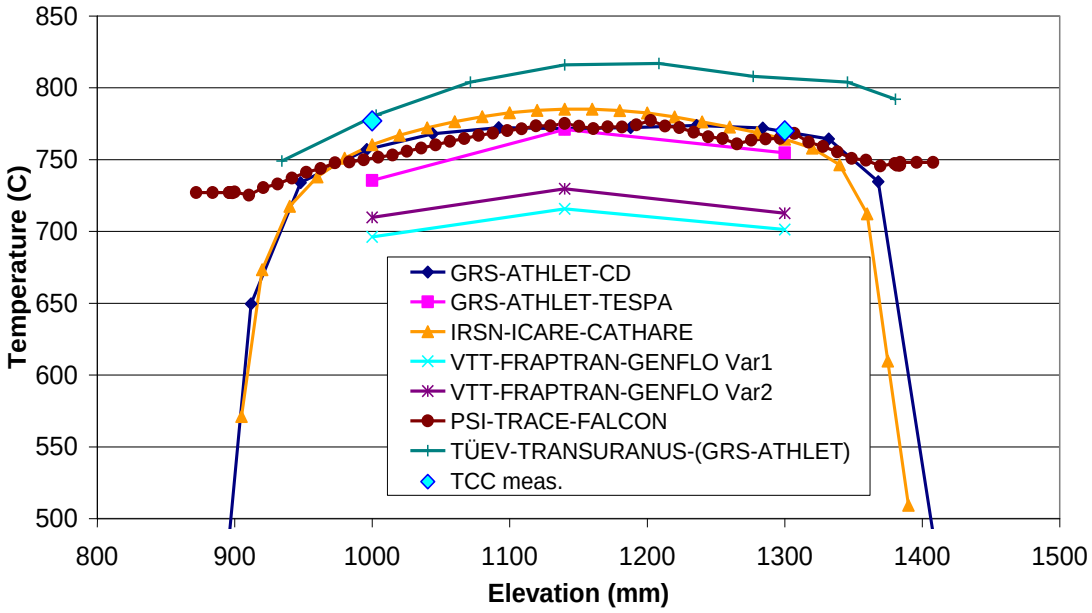

Fig. 7 – Temperature profile at burst

The calculated heater temperatures deviated quite much from the measured values both upwards and downwards, see Fig. 8. One of the possible reasons for this could be incorrect definition of the emissivity of the heater surfaces. Looking at the diversity in the rates of cooling-down, it could be also due to the incorrect heat capacity of the elements or incorrect temperature of the wall of the flask assumed in the calculation.

4.4 Strain

The calculated strain profiles all showed larger strains than measured (Fig. 9). Most likely, the strain obtained in the experiment would have been larger, had the rod not failed prematurely in the thermocouple weld area. The maximum strain was calculated and measured to be in the middle of the rod. The different shape of the PSI curve was due to calculation instability. The problem was subsequently fixed.

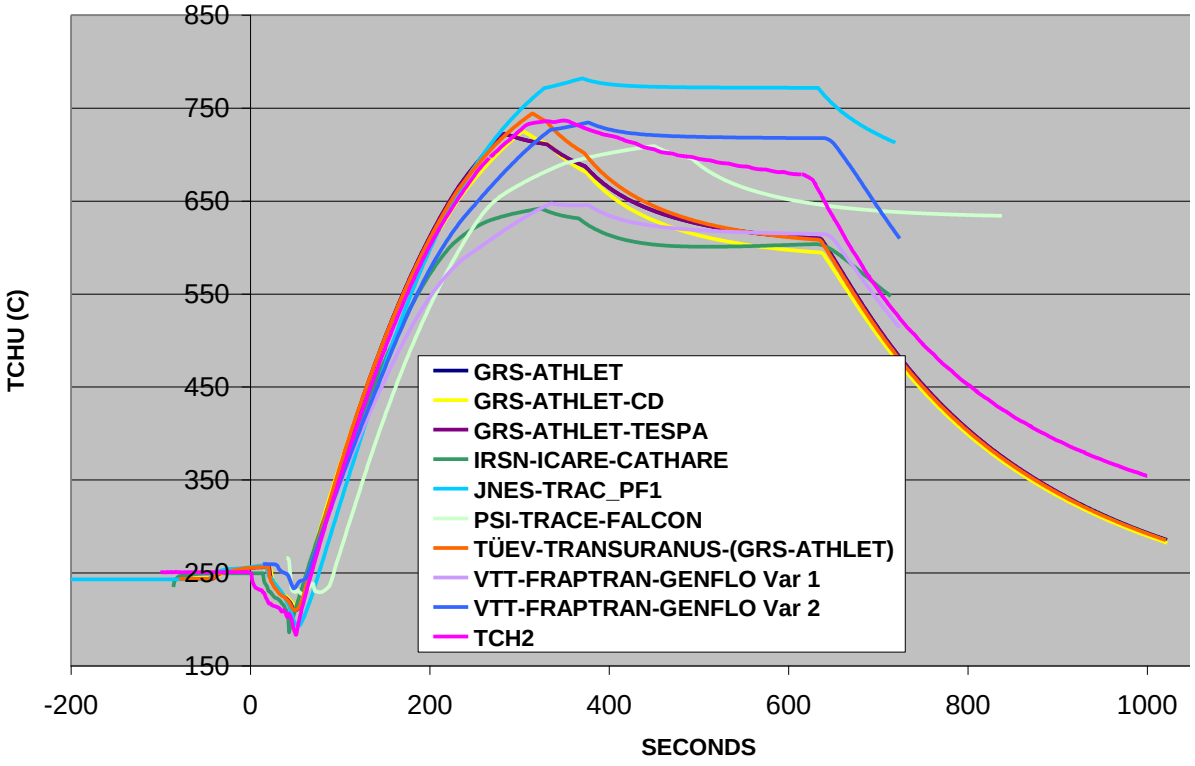

Fig. 8 - Heater temperature in time (adjusted)

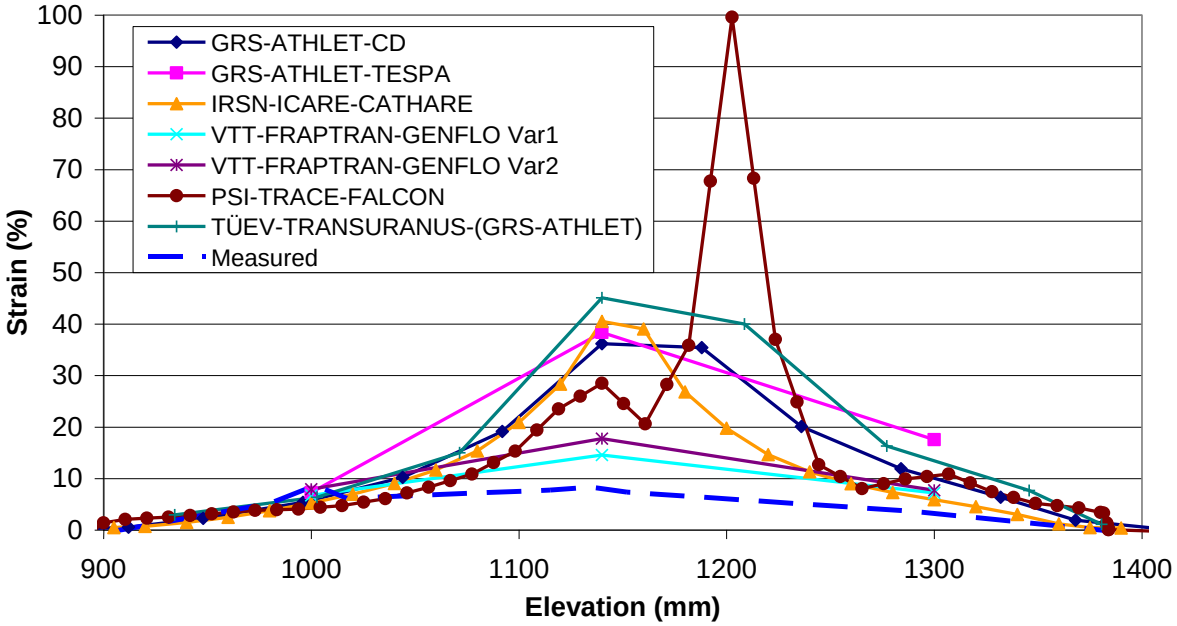

Fig. 9 – Strain at burst for blind calculations

5. POST-TEST CALCULATIONS, PHASE I

In this phase, participants were provided with the in-pile results from the test and asked to improve the models if necessary to obtain agreement with the experimental results.

5.1 Pressure behaviour

The rig pressure behaviour during blow-down was modelled well by most of the codes for which pressure was not used as an input variable; see Tab. 2 and Fig. 10.

Tab. 2 – Summary of post-calculations, phase 1

	Blow-down time (s)	Burst (s)	From TCCmin to burst (s)
GRS-ATHLET-CD		No prediction	
GRS-ATHLET-TESPA		No prediction	
IRSN-ICARE-CATHARE	34	291	257
PSI-TRACE-FALCON	47	258	211
TÜV-TRANSURANUS	47	269	222
MEASURED	48	267	219

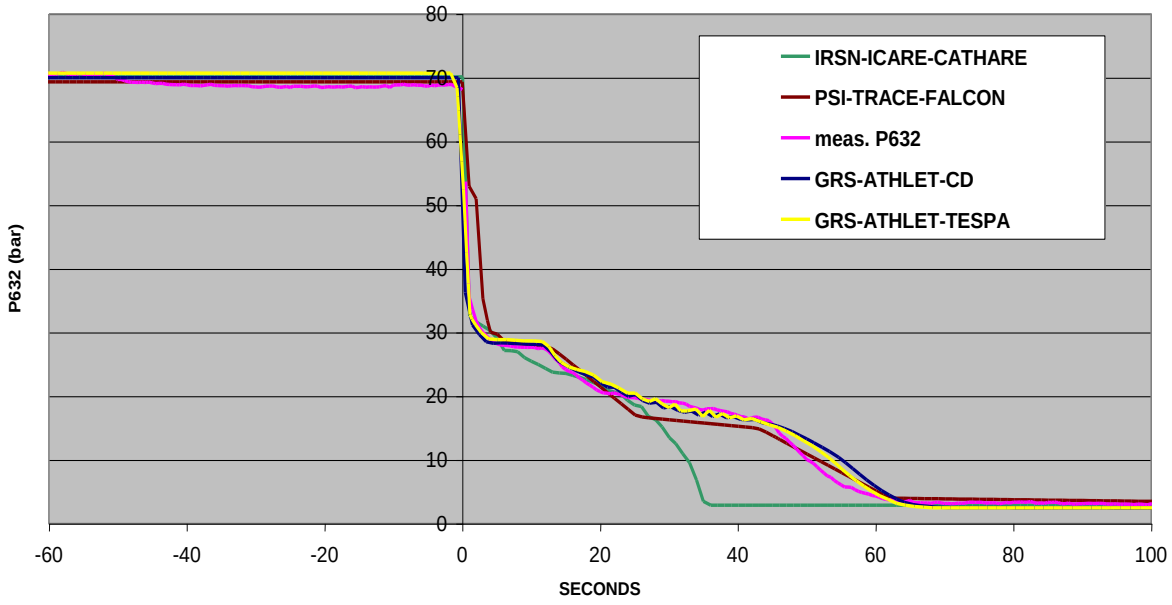

Fig. 10 – Rig pressure drop at blow-down

5.2 Ballooning and rod failure

The calculation of the time of ballooning and failure was significantly improved from the blind calculation. All codes predicted the burst to occur closer to the measured time than in the previous round, see Tab. 2 and compare Fig. 11 vs. Fig. 6.

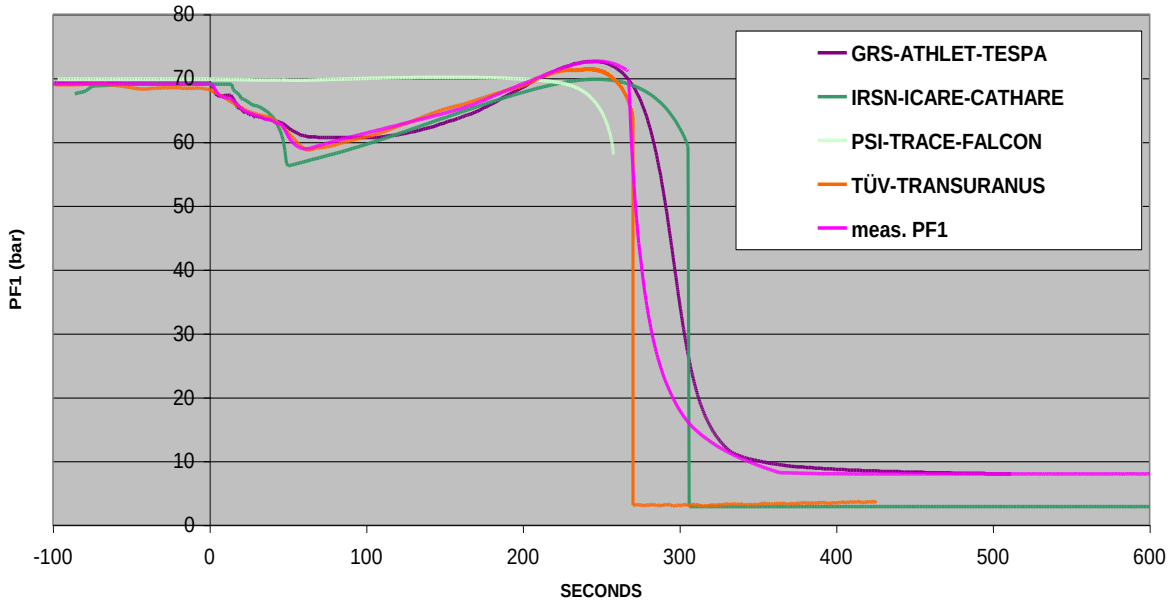

Fig. 11– Pin pressure, fixed to start of heat-up (adjusted)

5.3 Temperatures

The cladding temperatures were modelled quite well again (Tab. 3 and Fig. 12). The calculated cladding temperature profiles at burst time were slightly more symmetric than in the blind calculations. It was not tried to reproduce the measured bottom heavy profile, see Fig. 13.

Tab. 3 - Maximum temperatures

	TCCL	TCCM	TCCU
GRS-ATHLET-CD	852.8	835.6	824.8
GRS-ATHLET-TESPA	781.4	790	786.4
IRSN-ICARE-CATHARE	830	843	829
PSI-TRACE-FALCON	842.8	865.4	849.6
TÜV-TRANSURANUS	837.3	866.9	812.7
MEASURED	837	-	820/822

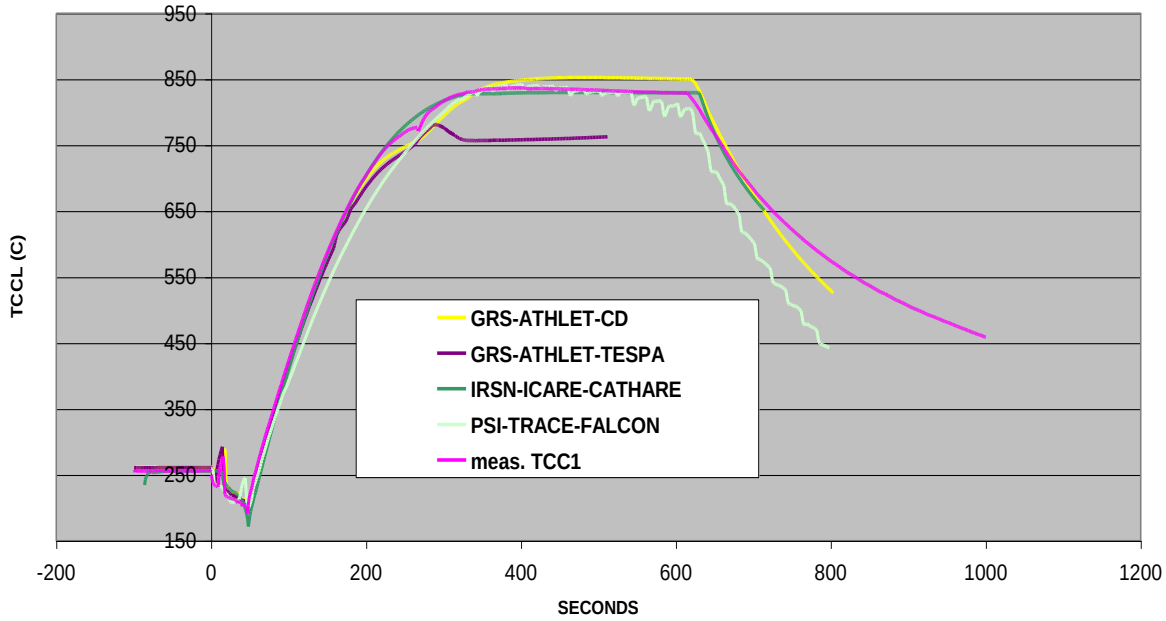

Fig. 12 – Evolution of cladding temperature in time (adjusted)

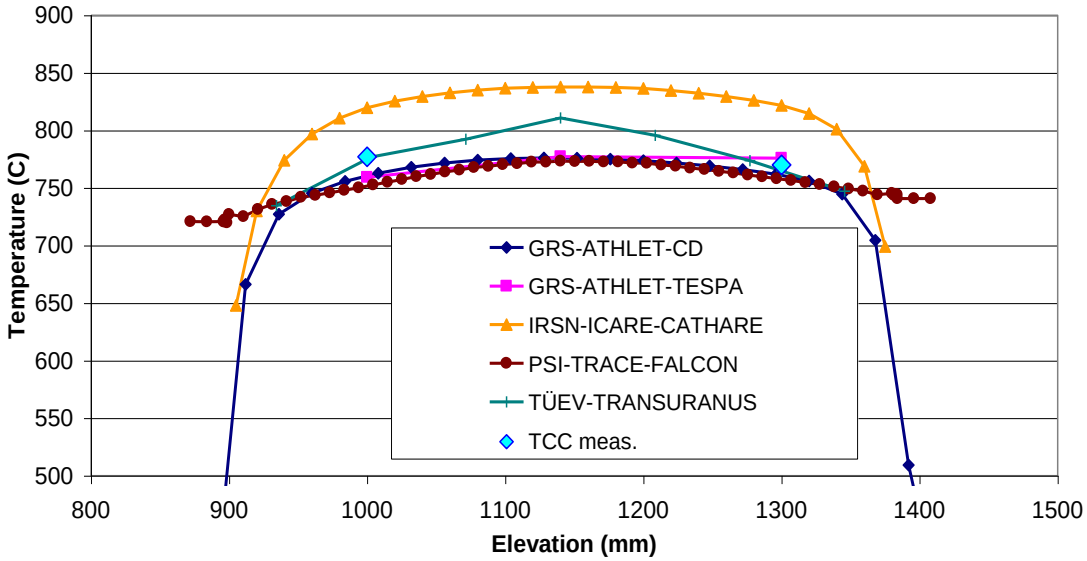

Fig. 13 – Temperature profile at burst – post calculations 1

5.4 Strain

Also the calculated strain profiles were more symmetric than in the first calculations. The maximum was calculated, similar to the measurement, at the middle of the rod, see Fig. 14. The calculated strains were again larger than measured, as expected.

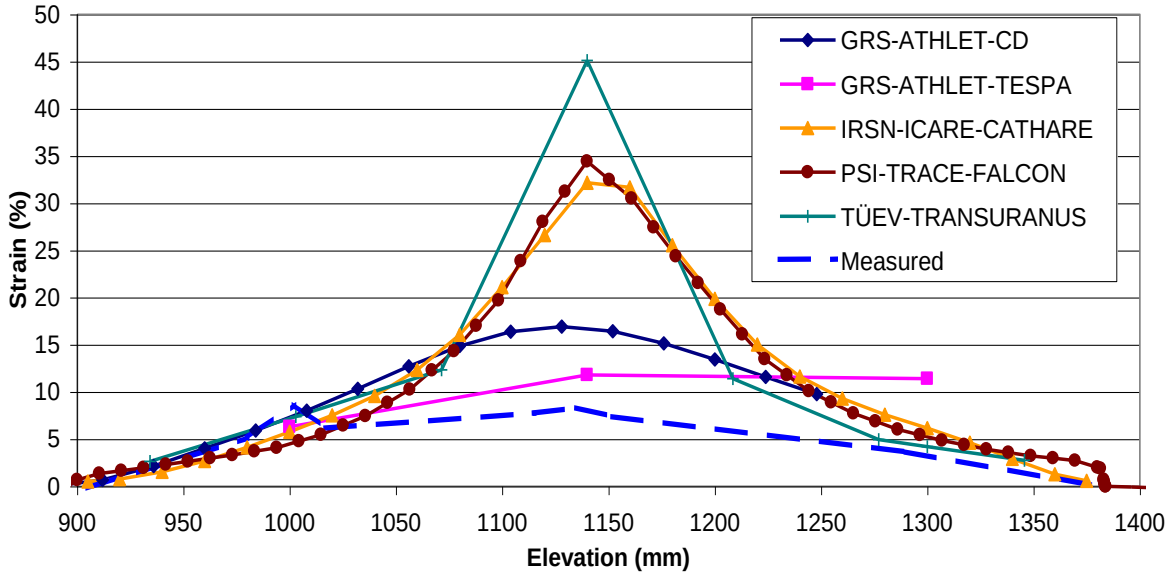

Fig. 14 – Strain at burst for various codes

6. POST-TEST CALCULATIONS, PHASE II – UNIFIED BOUNDARY CONDITIONS

In this phase, the calculations were repeated using a cladding temperature distribution calculated with ATHLET-CD at GRS.

6.1 Pressure behaviour and strain

The rig pressure behaviour during blow-down was modelled with all codes similar as in the 1st phase of the post-test calculations. The ballooning and burst times were not calculated as close to the measured values as without the unified boundary conditions, see Tab. 4.

Tab. 4 – Burst time predictions vs. measured value

CODE	BURST TIME (s)
GRS-CD	No prediction
TÜV-TRANSURANUS	305
PSI-FALCON	245
CEA-METEOR	285
IRSN-ICARE	356
MEASURED	267

Although the same axial cladding temperature distributions during the test were used in all calculations, there was discrepancy in the calculated strain profiles, see Fig. 15. While the comparison with the measured data is misleading (the balloon did not fully develop because of premature cladding failure at a weak spot introduced by cladding surface thermocouple welding), the spread among the calculated strains themselves indicates room for model improvement. Reasons for the discrepancies could be differences in axial nodalisation and the criteria used for defining cladding burst.

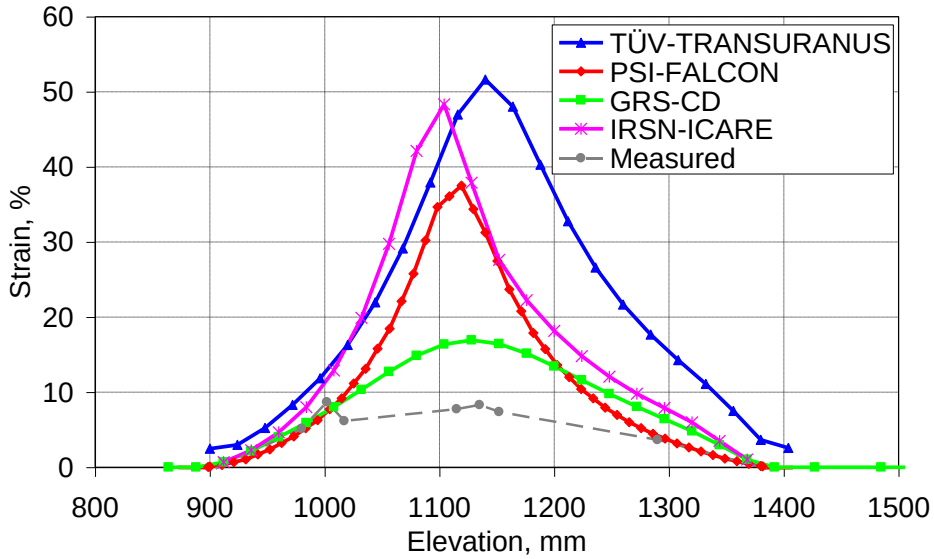

Fig. 15 – Axial strain profile at time of burst

7. BENCHMARK II - TEST EXECUTION AND PRINCIPAL OBSERVATIONS

Since IFA-650.3, when executed, did not produce the expected ballooning and fuel relocation, it was decided to continue the benchmarking with tests 650.4 and 650.5, this time as post-test calculations. Only four codes participated in Benchmark II.

In the following sections, the main outcome of the tests is briefly described.

7.1 Measurements and observations – IFA-650.4

IFA-650.4 was conducted on April 25, 2006 as repetition of 650.3. The fuel, provided by Framatome ANP, had been irradiated in a commercial PWR to 92 MWd/kgU burnup.

The experimental arrangements of the fourth test were similar to the preceding LOCA tests (see section 2.1), but cladding thermocouples were only attached at the upper end (TCC1 and TCC2). The target temperature of 800 °C was achieved, and cladding burst with fuel relocation occurred between 770-780ºC. Measured cladding and heater temperatures and heater power are shown in Fig. 16.

The temperature at the time of burst (336 s after blow-down) at TCC1 was 786 ºC and 784 ºC at TCC2. The temperature increase rates at TCC1 and TCC2 decreased prior to the burst, probably due to ballooning.

The cladding thermocouples cooled gradually after the burst to ≈600 °C at the start of the spray. The spraying was started 230 seconds after the cladding burst was detected in order to avoid disturbance from the spray in interpreting the signals and specifying the phenomena after the burst. The first spray pulse was 12 seconds, but after this the spray was applied as 0.5-second pulses every 20 seconds. The spraying enhanced the cooling, and the measured cladding temperature had dropped to ≈500 °C when the test was terminated by a slow scram 50 seconds after start of the spray or 617 seconds after the start of the test.

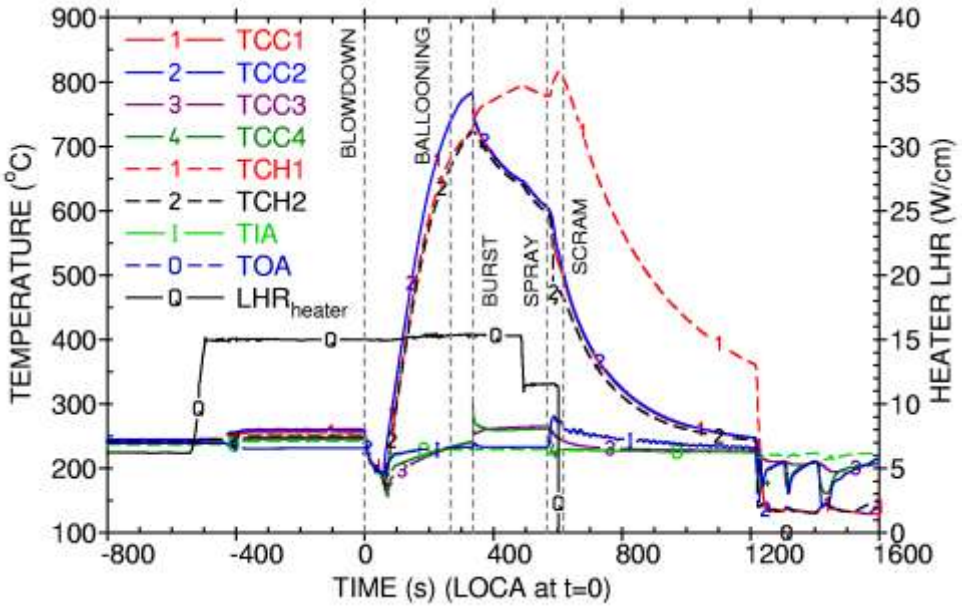

Fig. 16 - Cladding (TCC), heater (TCH), coolant inlet/outlet (TIA/TOA) temperatures and heater power during IFA-650.4

The pressure maximum was measured at 264-267 s after the beginning of the LOCA, i.e. ballooning probably started at this time, 70 seconds before burst. Cladding burst was detected 336 s after the start of blow-down. The indications of cladding burst can be seen in Fig. 17. The fast rod pressure drop starts at 366 s. At the same time a response is seen in the elongation signal. Also the gamma monitor on the blow-down line reacts to the burst, but 50-60 s later. The measured activity was of the same order as in IFA-650.3.

The response of the cladding and heater thermocouples indicated in-core fuel relocation. As there was no more fuel producing heat at the top of the rod, the temperatures measured with the upper thermocouples TCC1, TCC2, and TCH2 started to decrease, whereas the lower heater thermocouple TCH1 showed increasing temperature after the burst.

After the test, the fuel relocation was verified by gamma scanning which showed that about 19 cm of the original fuel stack was missing from the top of the rod and had dropped to the ballooned region at the mid-height of the rod and also to the bottom of the flask (Fig. 18).

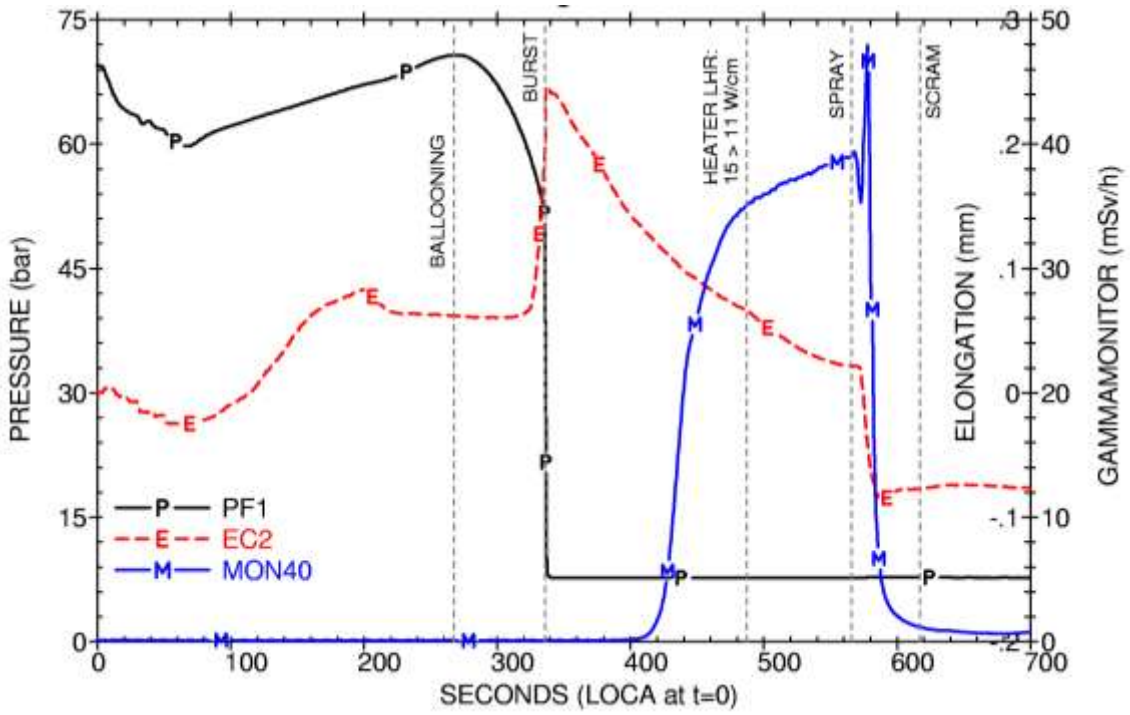

Fig. 17 - Cladding burst indications in IFA-650.4

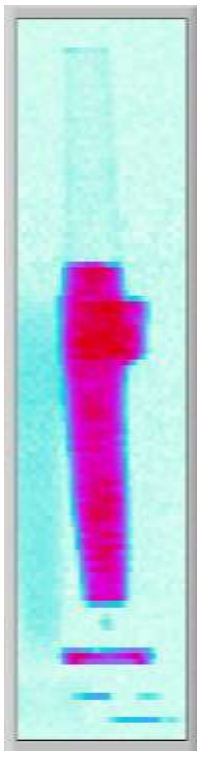

Fig. 18 - Post-test appearance as seen by gamma scanning

7.2 Measurements and observations – IFA-650.5

IFA-650.5, the third test with pre-irradiated fuel in the Halden Project LOCA test series, was conducted on October 23, 2006. The fuel rod provided by Framatome ANP was a sibling rod of the one used in IFA-650.3 and had a burnup of 83 MWd/kgU.

The experimental arrangements of the test were similar to the preceding LOCA tests. The target peak cladding temperature (PCT), 1100 °C, was achieved and cladding burst occurred.

The rig instrumentation was similar to IFA-650.4, except for one additional heater thermocouple at the bottom of the rod and one cladding thermocouple at the bottom of the rod, in addition to the two at the top. However, TCC2 at the top of the rod did not attach correctly.

The measured cladding and heater temperatures and heater power are shown in Fig. 19.

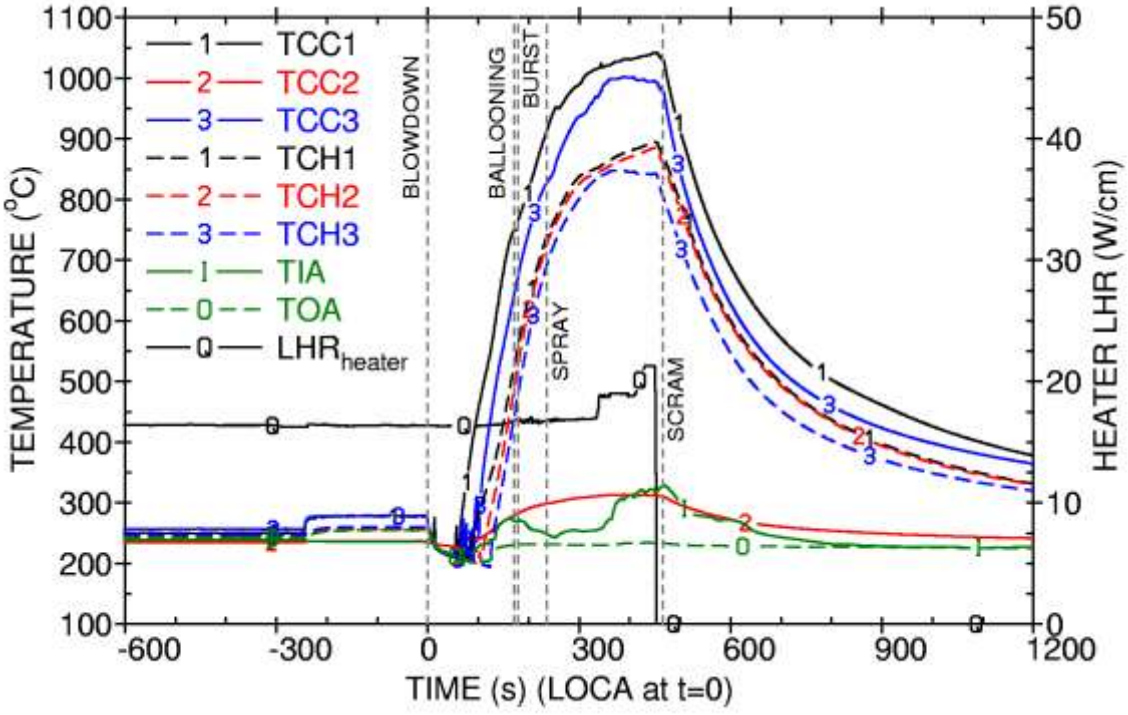

Fig. 19 - Cladding (TCC), heater (TCH), coolant inlet/outlet (TIA/TOA) temperatures and heater power during IFA-650.5

A temperature maximum of ≈1040 °C was measured with TCC1 at the bottom of the rod just prior to the scram. If the axial power profile is used for estimation of a peak temperature, a PCT value (≈1080 °C) close to the target is obtained. The cladding thermocouples showed increasing temperatures throughout the test until scram.

Cladding burst was detected 178 s after the start of blow-down. The indications of cladding burst can be seen in Fig. 20 as a rod pressure drop and a step change of the elongation signal. The gamma monitor on the blow-down line reacts to the burst about 15 s later. The measured activity was of the same order as in IFA-650.3 and IFA-650.4.

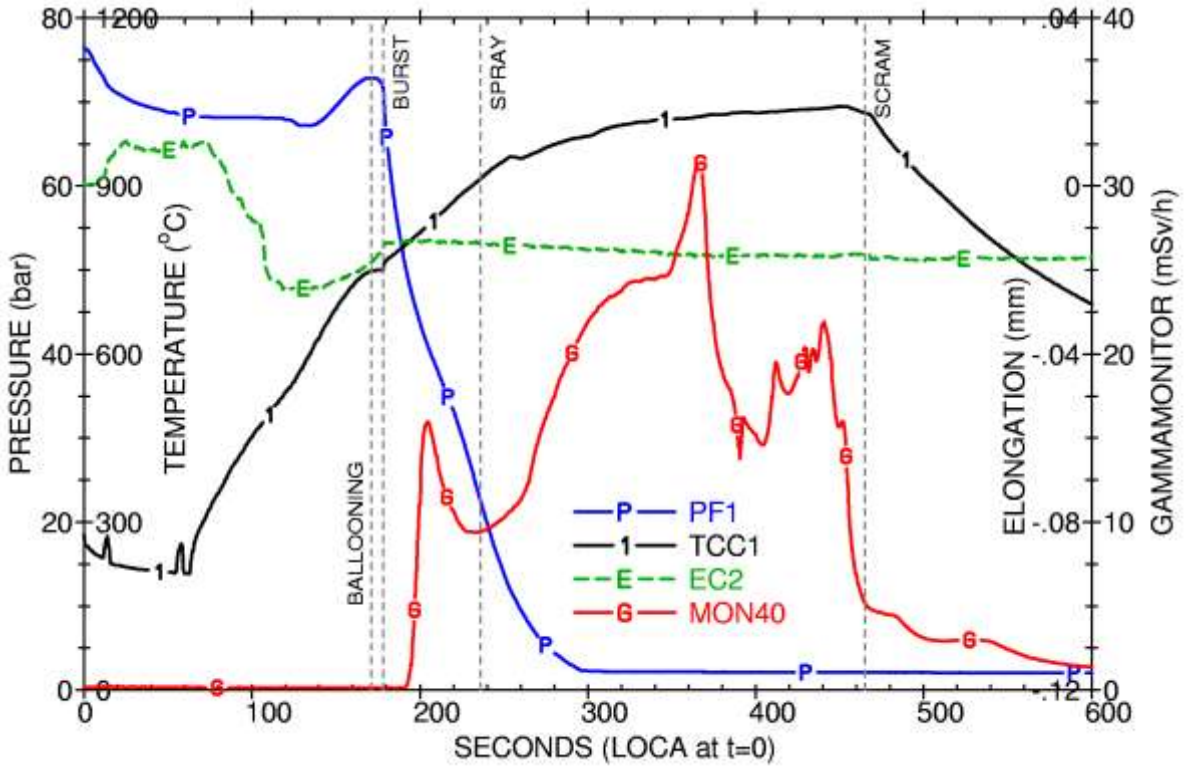

Fig. 20 - Cladding burst indications in IFA-650.5

The measured maximum pressure prior to ballooning and burst was 72.9 bar. The pressure maximum was measured 171 s after LOCA, i.e. ballooning probably started at this time, just 8 s before burst. Compared to the preceding tests, the rod pressure dropped very slowly after the burst.

Unlike IFA-650.4, no signs of fuel relocation could be deduced from the cladding and heater thermocouple signals. After the test, the absence of fuel relocation was verified by gamma scanning. However, also in this test some fuel was detected at the bottom of the flask.

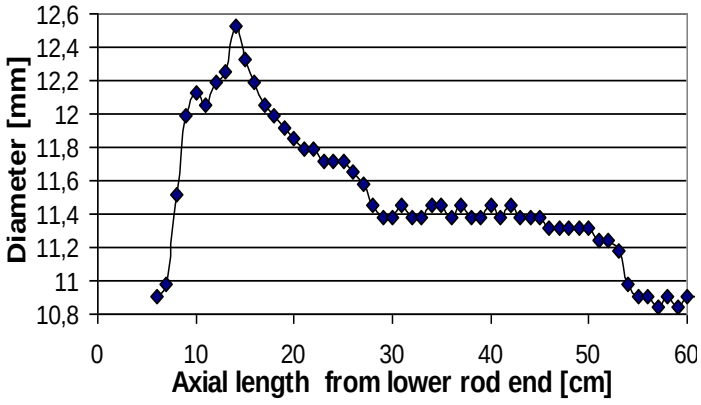

Fig. 21 - Cladding distension, rod 5

Fig. 21 shows the distension of rod 5 as measured by PIE. It appears that the upper half of the fuel rod was less affected by the transient, as indicated by the smaller distension over a length of about 25 cm. Since the cladding maintained good contact with the fuel, a restriction against gas flow remained in the upper half which is probably the cause of the slow pressure drop and small ballooning. Analysing the pressure drop data, it could in fact be verified that the gas permeability of the less distended part was similar to the permeability of high burnup fuels studied in the Halden experimental program using the technique of "hydraulic diameter measurement". Thus LOCA analysis codes can draw on many data for gas flow model verification.

8. RESULTS OF CODE CALCULATIONS

Four codes continued the benchmarking with Phase II comprising the tests 650.4 and 650.5. Emphasis was put on the treatment of IFA-650.4 which produced a large balloon and fuel relocation. For both experiments, GRS again provided a detailed set of temperatures calculated with the Athlet code in order to make it possible to apply the same boundary conditions to sensitive results such as extent and location of ballooning and time of failure.

8.1 Meteor (CEA)

Meteor is a fuel behaviour code and does not model the loop system. Therefore, for IFA-650.5, the external conditions (channel pressure and cladding temperature) were taken from the Athlet data. For IFA-650.4, the cladding thermocouples indications coupled with the profile determined in IFA-650.3 was used.

Before the calculation of the experimental LOCA phase, the base irradiation was modelled in order to calculate the transient with the correct free volume and input data for the modelling which depends on burn-up, porosities distribution, and fission gas distribution in the fuel. The results are shown in Fig. 22 to 25.

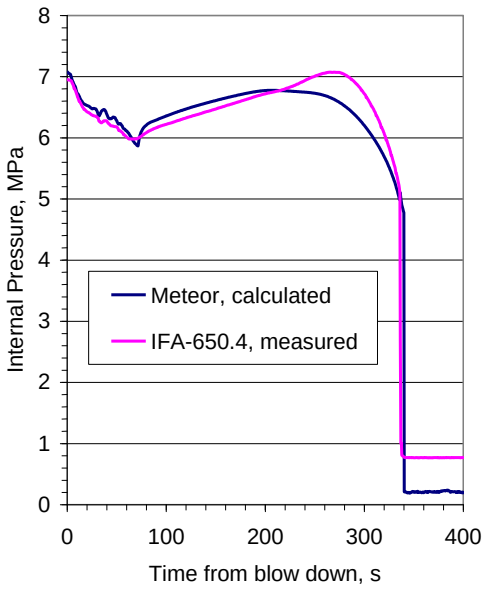

Fig. 22 - Pressure evolution in IFA-650.4 as calculated by Meteor

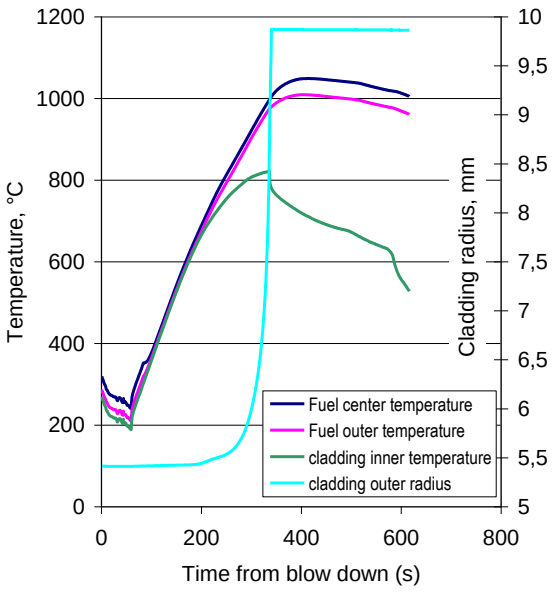

Fig. 23 - Temperature evolution in IFA-650.4 as calculated by Meteor

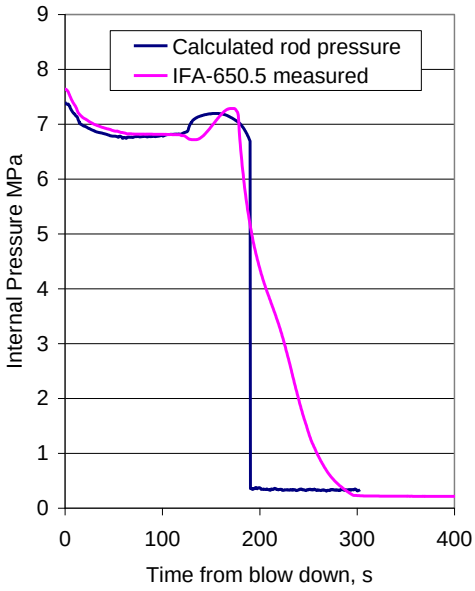

Fig. 24 - Pressure evolution in IFA-650.5 as calculated by Meteor

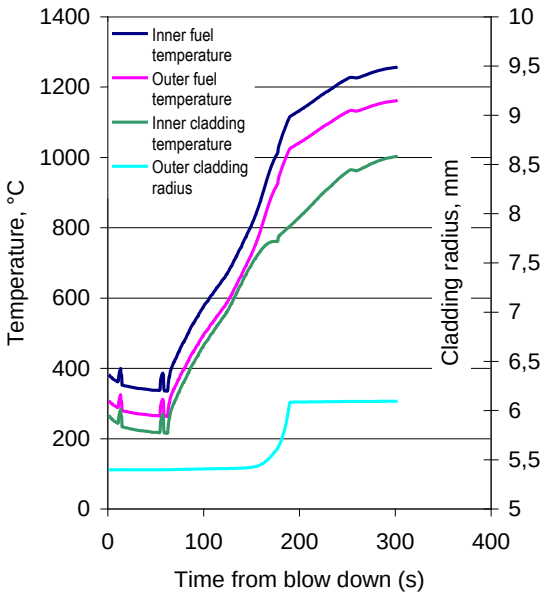

Fig. 25 - Temperature evolution in IFA-650.5 as calculated by Meteor

The cladding failure time is correctly calculated for IFA-650.4 (336s) and a little late for IFA-650.5 (195s). The cladding strain shows a quit good agreement with measurement for IFA-650.4 and IFA-650.5. The differences between the cladding strains at failure are attributed to the change of the mechanical and metallurgical properties due to the hydride concentration in the cladding. During the steady state irradiation, the external liner of IFA-650.4 induced a much lower corrosion thickness than for IFA-650.5.

In all cases, the calculation finds that fission gas release does not occur sufficiently early to contribute to the pressurisation of the rod.

8.2 ICARE/CATHARE (IRSN)

Preliminary calculations of the IFA-650.4 test were performed at IRSN with the fast running stand-alone module ICARE2 of the ICARE/CATHARE code [1], in which a specific model had been implemented to handle the slumping of fuel fragments in the rod balloon upon matching a pre-determined event in the transient such as the cladding burst. The fuel relocation model allows filling the free volume left between the fuel and the ballooned cladding with fuel particles slumping from upper elevations, with a user-input filling ratio and with allowance of some user-input fraction of fuel escaping from the rod.

However, the fuel relocation model has currently not yet been verified and validated against any experimental data. The results of the Halden LOCA tests, particularly IFA-650.4, are expected to provide the main source of results for the model validation.

The post-calculations of the IFA-650.4 test used the latest released version ICARE/CATHARE V2, which offers an improved coupling between the V2.5 version of the CATHARE thermal-hydraulic code and the latest version of the thermo-mechanic module ICARE2. Fig. 26 illustrates the schematization of the IFA-650 test rig that was used for the ICARE/CATHARE V2 calculations.

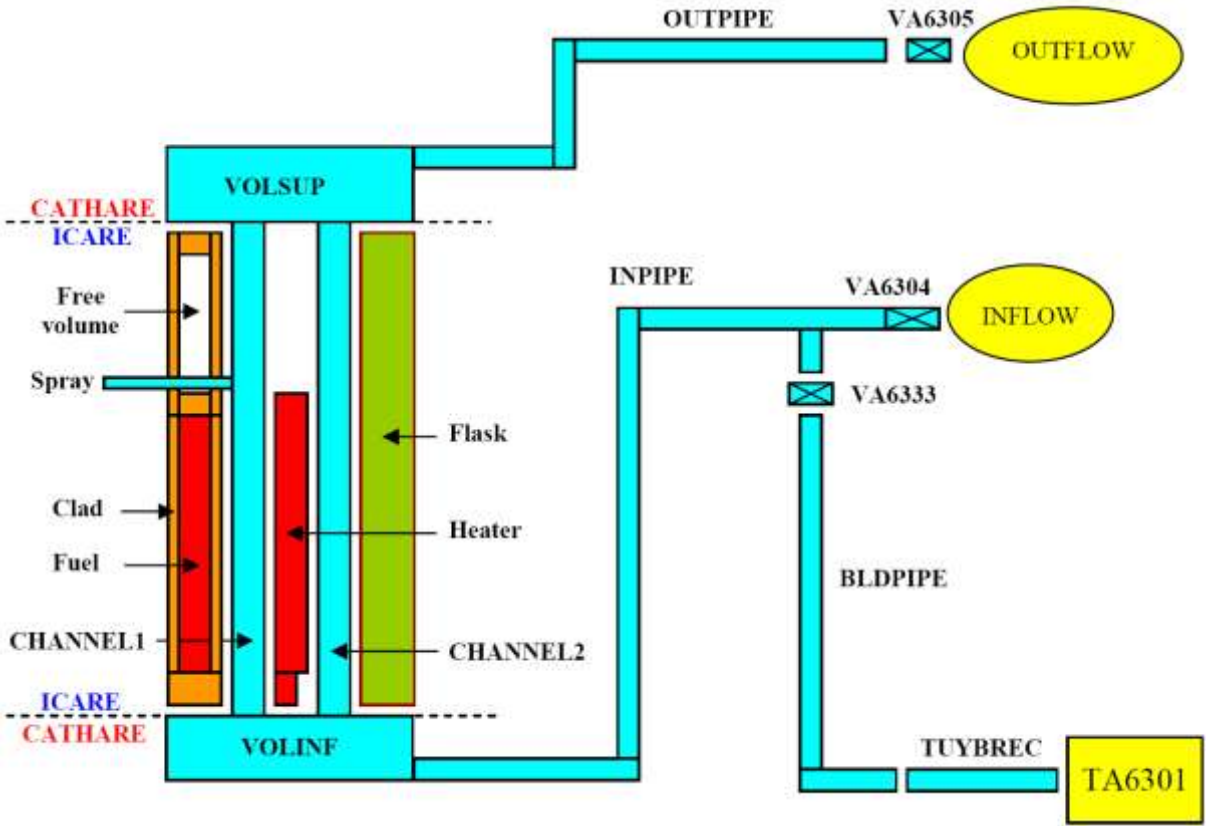

Fig. 26 - ICARE-CATHARE V2 Schematization of the IFA-650 Test Rig

In the calculation, the pre-transient phase was limited to 100 seconds, from -100 s at which the initial forced flow was stopped, enabling the establishment of the liquid flow natural circulation regime, until 0 s at which the blow-down was initiated by opening of the blow-down valves. The transient phase was limited to 550 seconds from the start of blow-down. No spray injection was considered in these calculated transients.

For the calculation results, the time required for blow-down was adjusted to the duration indicated by the measurements (beginning of heat-up). Fig. 27 compares the calculated and measured rod internal pressure variations, showing a good agreement in the pressure reduction associated with blow-down cooling and in the pressure increase during heat-up until vicinity of the cladding burst (experiment: 336 s / calculation: 316 s). This good agreement allows some confidence in the calculated burst conditions, although the burst strain value (90%) is slightly overestimated, possibly due to the use of as-received Zircaloy-4 mechanical properties for the calculation of clad strain and burst.

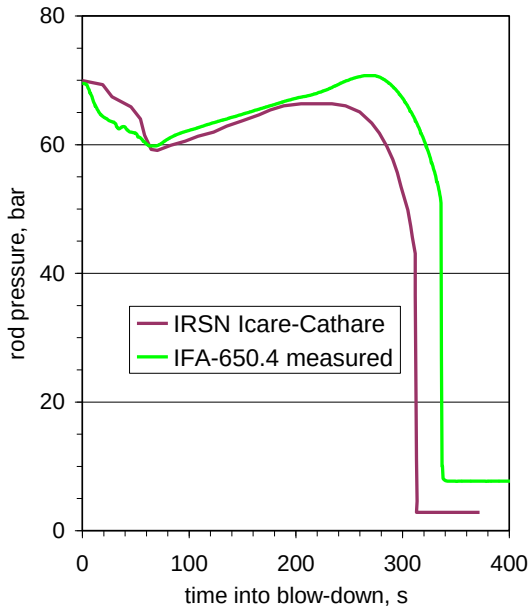

Fig. 27 - Pressure evolution in IFA-650.4 as calculated by ICARE-CATHARE

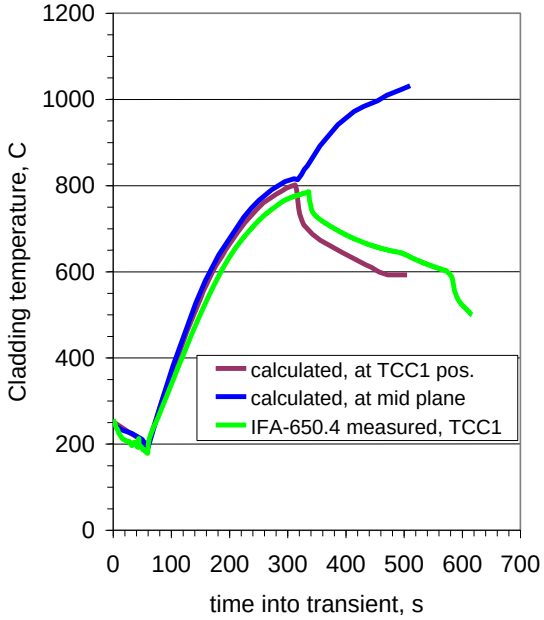

Fig. 28 - Clad temperature evolution in IFA-650.4 as calculated by ICARE-CATHARE

Fig. 28 compares the calculated vs. measured clad temperature variations at the upper TC elevation (+400 mm from fuel bottom, TCC1). Fuel relocation was imposed at clad burst with a 70% filling ratio of the clad balloon and with a provisional value of 20% of the slumped fuel escaping from the burst opening. The calculation shows a fair agreement with the measured TCC1 data until burst. The impact of fuel relocation on clad temperature is quite obvious and is correctly evaluated in the calculation as well.

Fig. 29 shows a comparison of the calculated vs. measured temperatures of the electrical heater at the lower (TCH1) and upper (TCH2) thermocouple elevations (+205 mm and 380 mm from fuel bottom, respectively). The figure shows again a good agreement at both TC levels. However, an underestimation up to 35°C at the lower TC elevation with a more gradual rise at burst than indicated by the measured data was observed in an earlier calculation. This underestimation was attributed to an insufficient heat transfer on the heater in the ballooned region where the distance between fuel rod and heater is considerably reduced, which makes the contribution of axial radiative transfer much more important than in undeformed geometry, and possibly due to no account in calculation of direct conductive transfer after contact between clad and heater.

The value of 70% chosen for the filling ratio of the ballooned cladding corresponds to the upper bound value of the few available data from PBF-LOC and FR-2 experiments [2] and may be considered realistic for high BU fuel such that of the IFA-650.4 rod (92 MWd/kgU).

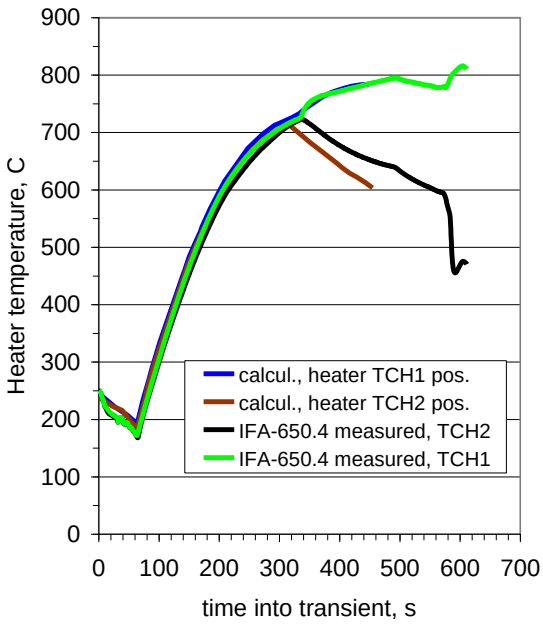

Fig. 29 - Heater temperature evolution in IFA-650.4 as calculated by ICARE-CATHARE

A lower value (50%) was also tested for comparison, and the results, not reported here, showed no appreciable difference on clad temperature variation and a rather larger underestimation on the heater temperature at lower TC position in comparison with the 70% filling calculation.

References

[1] V. Guillard, F. Fichot, P. Boudier, M. Parent, R. Roser, "ICARE/CATHARE : coupling: three-dimensional thermalhydraulics of severe LWRs accidents", 9th International Conference On Nuclear Engineering (ICONE-9), Nice-Acropolis, France, April 2001.

[2] V. Guillard, "Fuel relocation. Identification of areas where data may be needed", OECD Adhoc LOCA meeting, Paris, 27-28 June 2006.

8.3 ATHLET-CD (GRS)

The system code ATHLET-CD (**A**nalysis of **TH**ermal-hydraulics of **LE**aks and **T**ransients with **C**ore **D**egradation) is designed to describe the reactor coolant system thermal-hydraulic response during severe accidents, including core damage progression as well as fission product and aerosol behaviour, to calculate the source term for containment analyses, and to evaluate accident management measures.

For the application to the Halden LOCA experiments, the fuel pin was simulated with 22 equidistant nodes (spacing 24 mm over the length of 504 mm) between elevation 888 mm and 1392 mm. To simulate the ballooning as close as possible to the experimental findings, the measured internal fuel pin pressure (PF1) was taken as input data. In the simulation, the time of burst was 331 s (5 s too early).

In the IFA-650.4 test, the experimental results are consisted with the assumption of a symmetric axial temperature profile. The burst location is in the middle of the fuel rod. Therefore no artificial dripping of water from the top of the flask has been considered in the simulation.

Post-test gamma scans of the IFA-650.4 segment showed that the fuel of the upper 20 cm of the fuel rod had been axially relocated to the ballooned region of the fuel rod and to the surrounding of the rod. ATHLET-CD uses a fill factor which is defined as the ratio of the volume filled by relocated fuel to the volume increase by the ballooning of the fuel rod at a given axial position. A fill factor of 1.0 means then that the total added volume by the balloon is filled with fuel relocated from above whereas a fill factor of 0.0 means that no fuel was added.

PIE showed that the filling ratio of the ballooned region is about 40 %. Considering the widening of the fuel rod due to the ballooning, the amount of fuel per unit length inside the balloon is about the same as is it was before the ballooning. Therefore, the simulation is based on the assumption that the entire amount of fuel axially relocated during the transient is released to the surroundings of the fuel rod (fill factor = 0.0). It was assumed that the fuel relocates instantaneously at the time of the cladding burst (t = 336 s).

The fuel relocation has been simulated by setting the power release of the fuel to zero for axial positions of the fuel rod found empty in the gamma scans. This power distribution is solely suggested by the post test examinations from cross-sectional cuts at axial positions close to the burst area. Also the heat capacity of the fuel has been set to a very small value (1 % of the original value to avoid numerical problems) to simulate the fuel relocation.

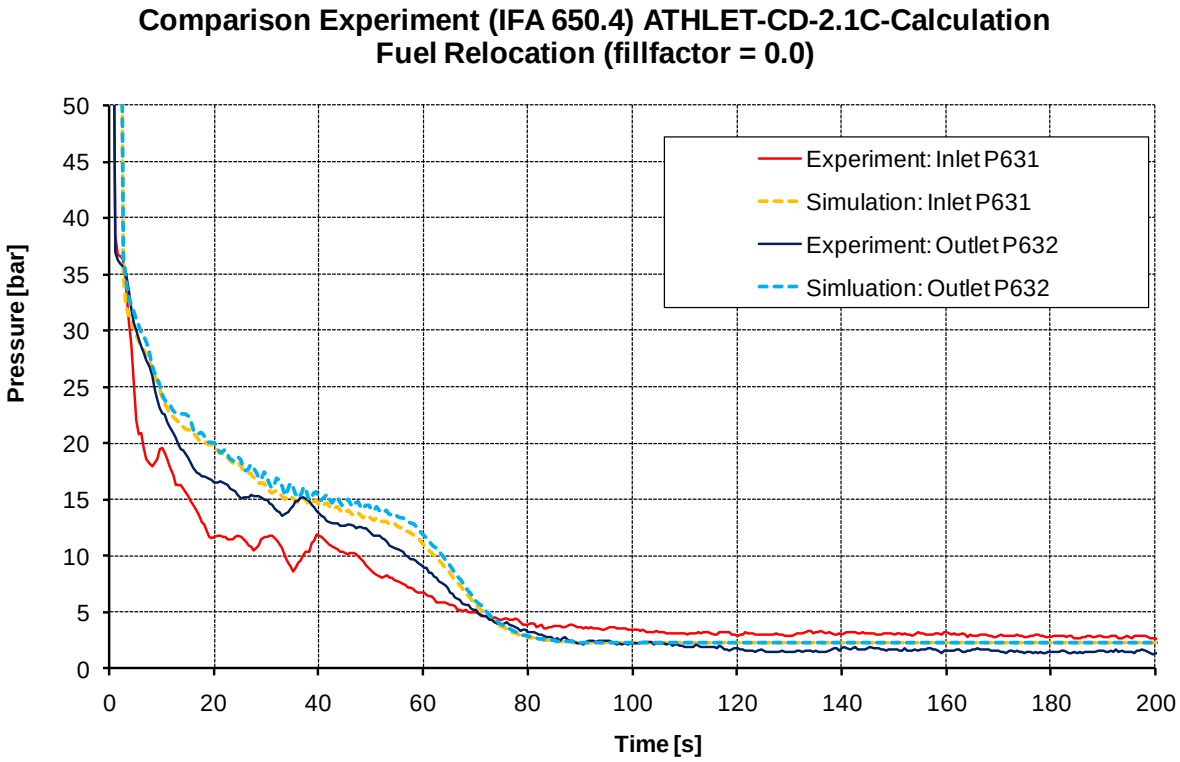

Fig. 30 - Pressure at inlet and outlet of the test section

As can be seen in Fig. 30, the time of the blow-down is reproduced consistently with the experiment. Also the pressure at the inlet and the outlet of the pressure flask is simulated with a reasonable accuracy. The pressure drop over the flask (ca. 5 bar) cannot be predicted correctly. In IFA-650.5, this pressure drop is even higher (ca. 10 bar) which could be explained by the added filters. Because this pressure drop does not significantly affect the relevant thermal-hydraulics, no further effort has been spent on this topic.

The simulation of the cladding temperature TCC fits well to the experimental results. During the period of the blow-down, the heat-up of the fuel rod and the period after the fuel rod burst compare well with the experimental results. The start of the spray at about 566 s is not simulated, but the scram at 617 s is.

In Fig. 31, the cladding temperature TCC at the position of the temperature sensor in the experiment (h = 0.4 m) and the temperature at the centre of the balloon (h = 0.25 m) is shown. There the temperature increase continues after the fuel rod burst until the reactor is scrammed.

The temperatures at the positions of the heater thermocouples show a difference of about 30 K at the time of the burst. The overall behaviour is simulated consistently compared to the results of the experiment.

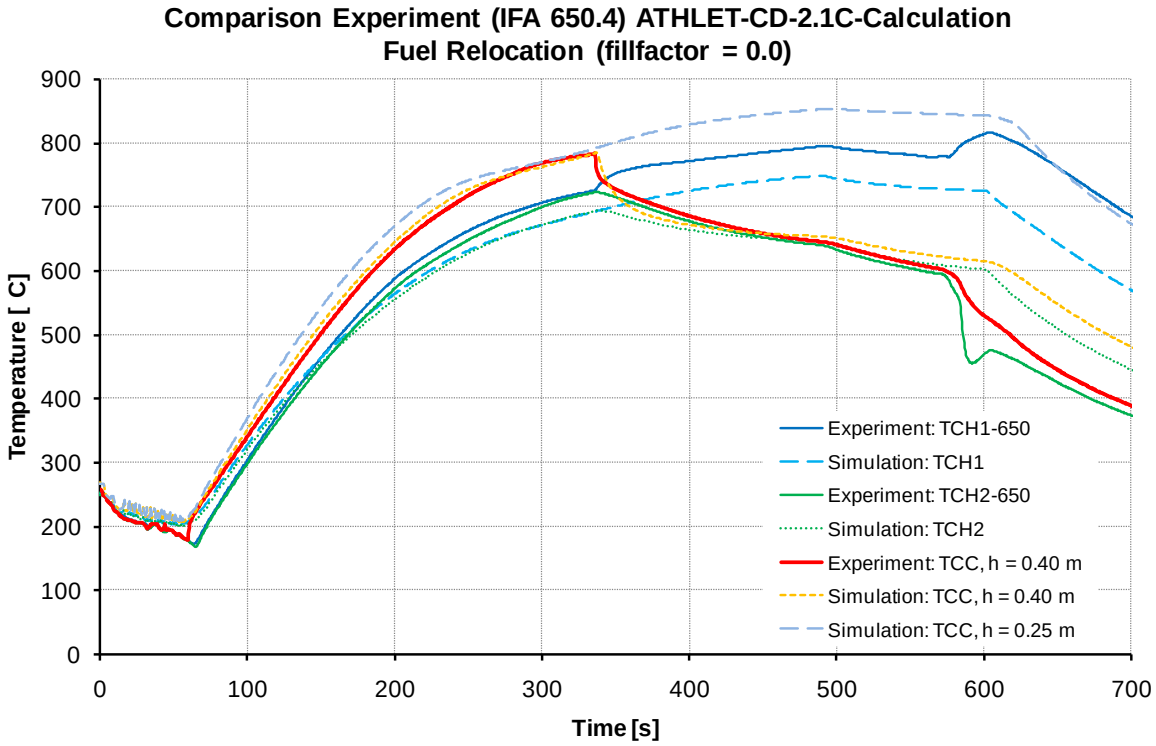

Fig. 31 - Temperature development in IFA-650.4

The case of IFA-650.5 was handled in a special way. The observed skewed axial temperature profile may have been caused by dripping of water from the top of the pressure flask onto the fuel rod. This was simulated by a variable spray flow. The amount of the spray flow was adjusted to best fit the simulation results to the two temperature measurements on the fuel rod (TCC1 and TCC2), Fig. 32.

The calculated axial temperature profile at the time of the burst shows a good agreement with the reported results of the experiment (±10 K), Fig. 33. Also the location of the burst agrees well with the simulated position showing the highest temperature (h = 984 mm).

All simulations were conducted without considering relocation of the fuel inside the cladding.

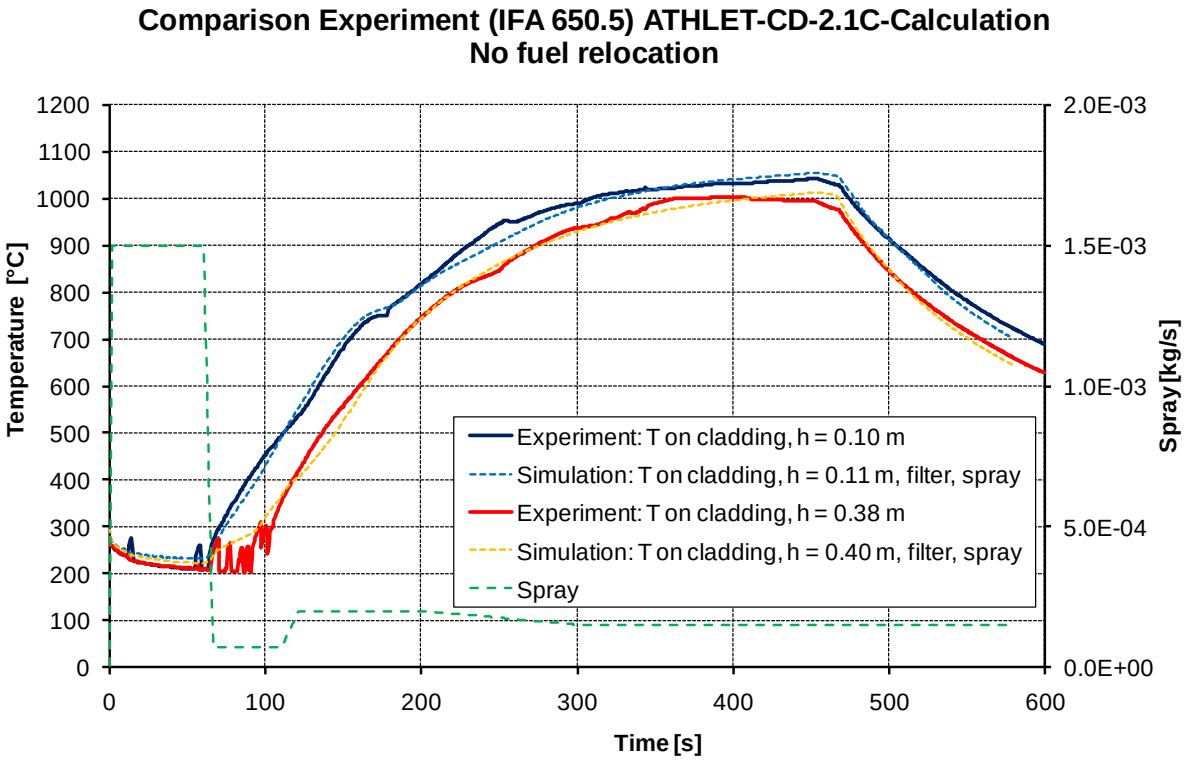

Fig. 32 - Temperature development in IFA-650.5

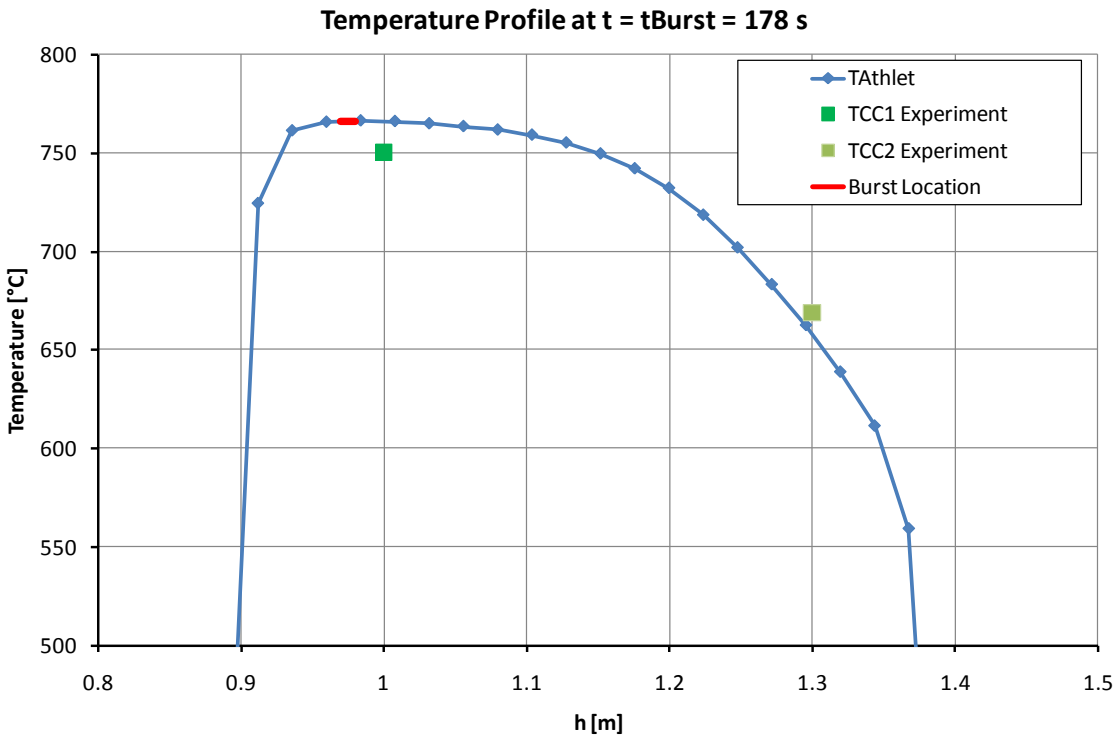

Fig. 33 - Temperature profile in IFA-650.5 at time of burst

8.4 FRAPTRAN-GENFLO (VTT)

The FRAPTRAN-GENFLO code system is a parallel application of advanced thermal hydraulics and detailed fuel performance descriptions with models developed by VTT. This section is a summary of RESEARCH REPORT VTT-R-01738-09 "Halden IFA-650.4 LOCA Test Calculation with FRAPTRAN-GENFLO".

The original thermal hydraulic model of the IFA-650 loop calculation was made on the best understanding of the loop characteristics during forced flow, natural circulation and LOCA blow-down conditions. After the blow-down and fuel rod heat-up, the radiation heat transfer is adjusted in such a way that the stabilised temperatures of the rod and the electrically heated shroud agree with measure data, should there be no actuation of the spray. The holes between the inner and outer annular spaces are assumed to allow natural circulation of single-phase steam, whereby superheated vapour would flow upwards in the inner annulus and the cooled vapour down in the outer annulus.

Temperature calculation

The radiation balance is controlled by the emissivities of the rod and shroud surfaces. For the IFA-650.4 calculation, emissivities of 0.90 and 0.75 for the rod outer and heater inner surfaces, respectively, were assumed.

In the experiment, the cladding and heater thermocouples clearly suggest fuel relocation: the clad TC's that locate at the upper end of the rod show sharply decreasing temperatures, whereas by a heater TC near the balloon region, a strong increase is observed after the indication of cladding burst.

A parametric study was carried out to match the measured and calculated heater temperatures at the lower location by varying the rod power. The best agreement was obtained with a linear power of 2.0 kW/m. Heater temperatures are compared in Fig 34. If one had postulated that the balloon be filled with solid fuel, the power would have risen to 3 kW/m.

As for the cladding temperatures, the assumed zero LHGR makes the calculation follow the measured data fairly closely at the upper end elevation (Fig. 35). Fig. 35 also shows the calculated lower-end temperature (no measurement, no LHGR adjustment) and the distinctly increasing mid-elevation temperature (elevation of balloon in the calculation).

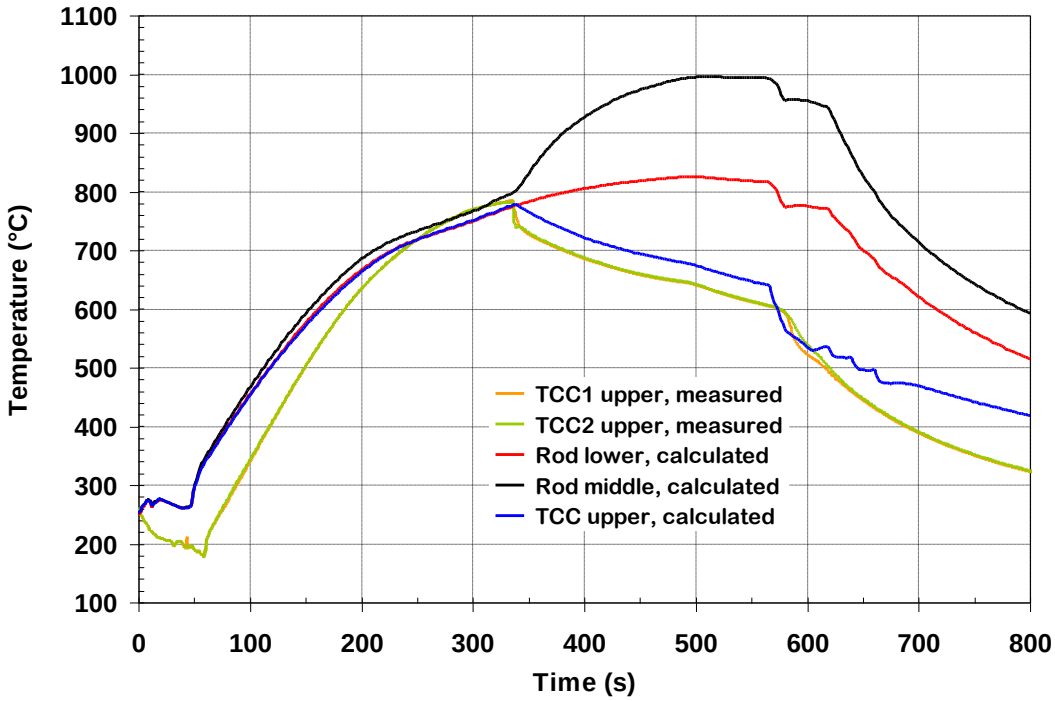

Fig. 34 - IFA-650.4 heater temperatures with assumed relocation effects

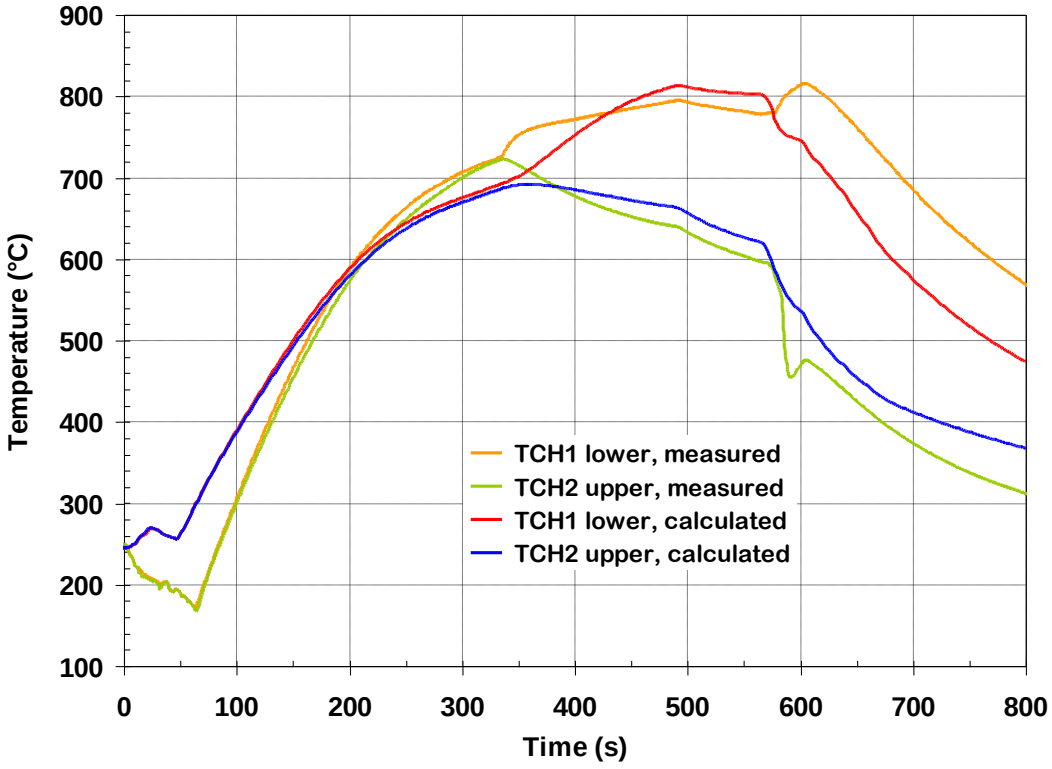

Fig. 35 - IFA-650.4 cladding temperatures with assumed relocation effects

9. COMPARISON OF RESULTS – BENCHMARK II

In this chapter, the main results of the code calculations are shown combined in overview graphs for comparison. Only IFA-650.4 is shown in this way since IFA-650.5 was not treated by all codes.

9.1 Rod pressure and time of failure

The comparison, Fig. 36, indicates various degrees of agreement with the measured data (the Athlet-CD results are not shown; they are identical with the measured pressure which was used as input).

- The pressure decrease during the blow-down phase and the following increase due to heating up the system is not rendered by Fraptran-Genflo.
- All codes are in satisfactory agreement with the evolution of decreasing pressure after onset of ballooning until rupture which is an indication of correct calculation of the balloon size.

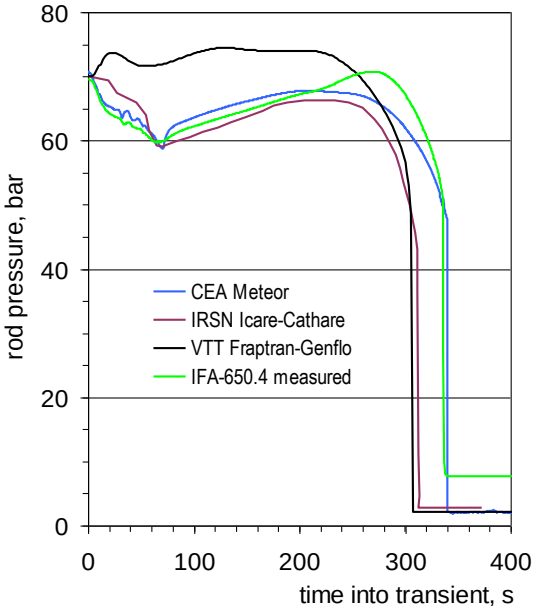

Fig. 36 - Rod pressure evolution in IFA-650.4 - measured and calculated

- The time of rupture, 336s, is best rendered by Meteor (340s), but the other results (Icare-Cathare 316s, Fraptran-Genflo 308s) are within an acceptable range of deviation.

9.2 Cladding temperature

Fig. 37 shows the comparison of the measured and calculated cladding temperatures at the position of the upper cladding thermocouple in IFA-650.4.

- All codes predict the initial, steep temperature rise after end of blow-down, although Fraptran-Genflo does not render the cooling associated with the blow-down.

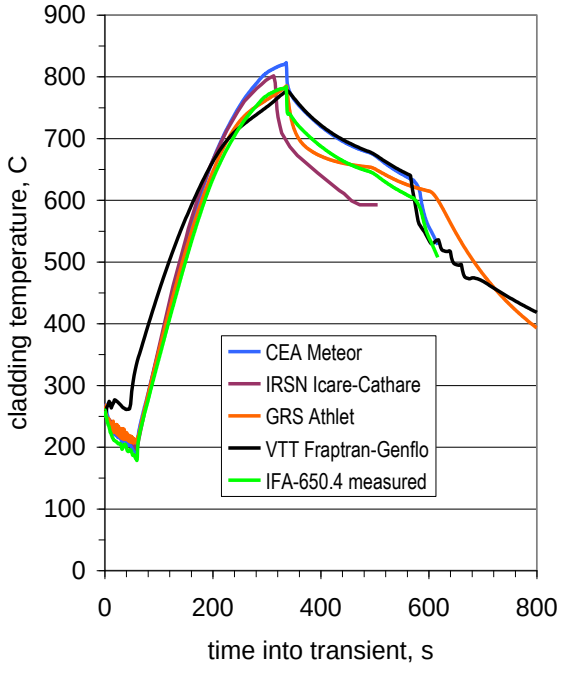

Fig. 37 – Cladding temperature evolution in IFA-650.4 - measured and calculated

- The peak temperature at the upper TC position, occurring at rupture, is reproduced well by all codes and agrees with the measurement within 35 degrees C (Meteor).

- All codes introduced a feature to consider the missing (relocated) fuel after clad rupture. The calculated temperature decreases are in overall agreement with the measurements, but the decrease calculated by Icare-Cathare is on the high side.

9.3 Ballooning strain

IFA-650.4 is characterised by quite large ballooning of the cladding, as intended according to the objectives of the test. This is mainly brought about by the uniform heating and circumferential temperature distribution. The calculated and measured cladding strain at the ballooning location is shown in Fig. 38.

- The code results are in good agreement with the measured maximum strain of about 62%.

- Meteor and Fraptran-Genflo agree in their prediction of the onset of ballooning at approximately 200 seconds into the transient.

- A comparison with the development of the rod pressure (Fig. 36) indicates that this onset is probably too early (the measured pressure starts deviating from the increase at about 260 seconds).

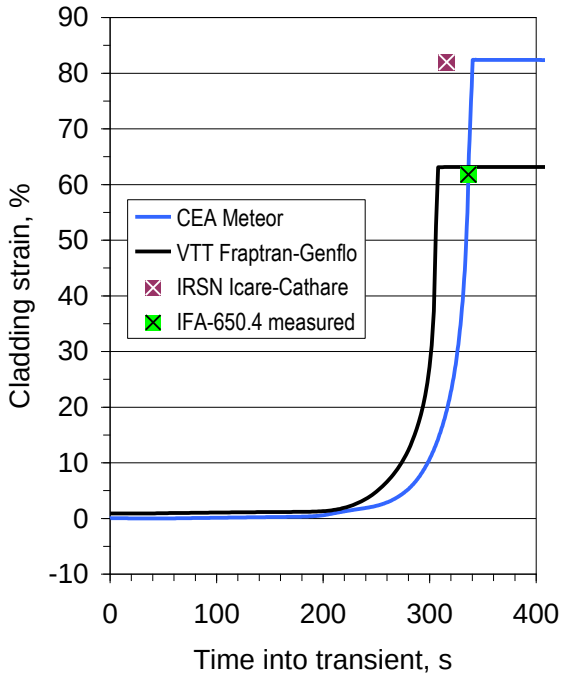

Fig. 38 – Cladding strain evolution in IFA-650.4 - measured and calculated

10. SUMMARY AND CONCLUSIONS

Several code benchmarks were conducted using data from the Halden LOCA test series for comparison. The benchmarks concentrated on the thermal and mechanical response of the fuel and cladding, including the effect of fuel relocation as one of the primary objectives of the Halden test series. The other objective, namely to investigate the extent of "secondary transient hydriding" on the inner side of the cladding above and below the burst region, was not addressed by the codes since the experiments were not conducted in the high temperature oxidation phase of the transient. This does not mean that secondary hydriding is not an important phenomenon with impact on LOCA safety criteria.

The first benchmark was implemented as three rounds of calculations starting with a blind pre-test calculation. The results differed amongst the codes and also between the calculation rounds.

In the first round, the codes underpredicted the time to burst. This was largely fixed in the second round of calculation where the agreement between predicted and measured burst time was good. In the third round of calculation using unified thermo-hydraulic boundary conditions, three codes overpredicted the time to burst.

The codes were able to render the dynamics of the fairly complicated experimental system in a satisfactory way as shown by the rig pressure drop (Fig. 5). The calculated heater temperatures showed a larger spread and deviation from the measured value, possibly due to sensitivity of the calculations to emissivity values, which was also observed when the codes were calibrated to the system with the commissioning runs.

Strain profiles at burst showed severe over-prediction of strain in all three cases in all codes. This is understandable since the experiment did not develop as foreseen and failed at a weak spot introduced by thermocouple welding. However, the spread of calculated ballooning strains even when uniform boundary conditions were applied indicates that the associated modelling can still be improved.

The second benchmark using data from the Halden LOCA series was completed by four codes: ATHLET-CD (GRS), Fraptran-Genflo (VTT), Icare-Cathare (IRSN), and Meteor (CEA). These codes participated in the first phase as well and contained modifications and improvements to be able to render the Halden experiments in a better way.

On average, the codes agreed reasonably with the experimental results.

Regarding rod pressure, the effect of ballooning causing the pressure to decrease was well calculated by the codes, implying that also the ballooning strain is calculated with a similar degree of agreement with the measured maximum strain of about 62%.

Also regarding time to failure at measured 336s, the results were within an acceptable range of deviation (308 – 340 s).

The most critical calculation is the cladding temperature since it is directly linked to the safety criterion limit of peak clad temperature and has a strong influence on cladding oxidation which is limited by the

ECR safety criterion. The peak temperature as measured at the upper thermocouple position in IFA-650.4 was reproduced well by all codes and agreed with the measurement within 35 degrees C. The codes were conservative in that the results were slightly higher than measured.

As an improvement, the codes introduced the effect of fuel relocation on cladding temperature. The principal effect seems to be well described as evidenced by Fig. 37. However, improvements regarding details of the temperature response to fuel relocation should still be sought since the codes will be used to evaluate a potentially critical part of a safety assessment.

That fuel relocation as seen in IFA-650.4 is not a singular occurrence was demonstrated with Halden LOCA test 650.9 carried out with 650.4 sibling fuel on April 17, 2009. The observations underline the importance that codes for LOCA analysis should be improved to model the relocation phenomenon and calculate the consequences on local cladding oxidation and embrittlement.

11. APPENDIX I – DESCRIPTIONS OF CODES PARTICIPATING IN BENCHMARK II

11.1 Meteor

Meteor is a mono-dimensional fuel performance application; it models the behaviour of LWR fuel rods in normal and incidental conditions. Its current version, V2, is validated for UO_2 and MOX fuel up to 70 GWd/tm with cladding Zy4 or M5 in PWR conditions.

It describes several aspect of the fuel rod evolution: thermo mechanics, fission gas behaviour and microstructural changes at high burn up.

The fuel rod is considered as a stack of axial slices for which a thermal analysis and an axi-symmetric, isotropic and 'generalised' plane strain analysis are performed.

Thermal aspect

The thermal behaviour is classically mainly driven by the heat transfer through the fuel cladding gap, the fuel conductivity and the radial distribution of power.[1]

Mechanical aspect

The model describes radial and axial cracks that appear as a result of the hoop or axial stresses exceeding the assumed fuel fracture stress. In a given slice, the fuel pellet is divided into meshes over which the mechanical properties are assumed to remain constant. Each mesh may take on four distinct crack related states, i.e. uncracked, radial crack open and axial crack closed, axial crack open and radial crack closed, radial and axial cracks open.

Fuel and cladding creep are modelled and treated implicitly. However, an iterative scheme is applied to converge over a time step on a value of $\dot{\varepsilon}/\sigma_e$, where $\dot{\varepsilon}$ is the creep rate and σ_e the Von Mises stress.[2] Fuel densification, fuel swelling (solid and gaseous) and thermal expansion are introduced explicitly in the analysis as components of the strain tensor.

[1] IAEA Seminar, Cadarache France, September 1998, Temperature calculation and the effect of modelling the fuel mechanical behaviour, P. Garcia, C. Struzik, N. Veyrier.

[2] Mono-dimensional mechanical modelling of fuel rods under normal and off-normal operating conditions, *Nuclear Engineering and Design, Volume 216, Issues 1-3, July 2002, Pages 183-201*. Ph. Garcia, C. Struzik, M. Agard, V. Louche.

Fission gas behaviour aspect

Considerable attention is paid to the fission gas behaviour and to the fuel microstructural changes due to increasing burnup.

In steady state conditions, two populations of gases are described: intragranular and intergranular. The intragranular gas diffusion is modelled. Trapping and resolution of gas atoms from intragranular bubbles into the matrix are taken into account as a corrective factor of the bulk diffusion coefficient of the fission gas. Intragranular bubbles density and radius are given by empirical correlations.

Intergranular gas is assumed to be contained in bubbles, their number being an empirical function of burn-up and temperature. After interconnection of bubbles, fission gas is released towards the free volume of the rod by percolation.

The rim built up is considered to be a balance between irradiation defaults accumulation due to local fission density and their thermal recovery.

In transient conditions, intragranular and intergranular bubbles are represented, and the evolution of their diameter is modelled, but their initial density is empirically assessed. The growing of these bubbles leads to transient fuel swelling.

LOCA description

To describe the LOCA conditions, models built on specific out of pile experiments have been introduced. Regarding the cladding, a model of cladding creep and failure coupled with the kinetics of phase transition of Zircaloy at high temperature has been developed from EDGAR experiments [[3]] and introduced in METEOR. These experiments consist of monitoring thermal ramp tests on pressurised tubes (fresh and hydrided). The failure time and the cladding strains are measured.

The fission gas behaviour in LOCA conditions has been modelled from GASPARD experiments (out of pile thermal test performed on fuel with burn up in the range 40-80 GWd/tm). These tests consist in monitoring ramp test on irradiated fuel with concomitant fission gas (Kr 85, Xe 133) release measurement[4]. The modelling introduced and validated in METEOR deals mainly with grain boundary opening under fracture or bubble gas interconnection. Then METEOR is able to describe the first part of the LOCA up to the cladding failure.

11.2 ICARE/CATHARE

The ICARE/CATHARE code has been developed by the IRSN within the framework of PWR safety analysis. It results from the coupling of the mechanistic severe accident code ICARE2 (developed by the

[3] «Influence of hydrogen content on the α/β phase transformation temperatures and on the thermal-mechanical behavior of Zy-4, M4 (ZrSnFeV) and M5TM (ZrNbO) alloys during the first phase of LOCA transient» Zirconium in the Nuclear Industry: 13th. International Symposium, (June 10-14 2001), Annecy,France J. C. Brachet, L. Portier, T. Forgeron, J. Hivroz, D. Hamon, T. Guilbert, T. Bredel, P. Yvon, J.P. Mardon, P. Jacques.

[4] Experimental and theoretical investigation of fission gas release from UO_2 up to 70 GWj/tm under simulated loca type conditions: The gaspard Program, Y. Pontillon et al., Proceedings of the 2004 International Meeting on LWR Fuel Performance, Orlando, Florida, September 19-22, 2004.

IRSN since 1988) with CATHARE2 thermal-hydraulics modules (0D, 1D and 3D), the CATHARE2 code being developed by CEA and co-financed by CEA, IRSN, EDF and AREVA-NP. It allows to calculate PWR and VVER severe accident sequences in the whole Reactor Coolant System (primary and secondary circuits).

Particularly, the computer code ICARE/CATHARE V1 was intensively used within the framework of the PSA2 of 900 MWe French PWR. This code was widely validated and was assessed on many accidental scenarios and by comparison with bundle experiments[5]. The results obtained were considered to be satisfactory and reliable up to the end of the early degradation phase. A full multi-dimensional modelling (covering both the fluid flow and the corium behaviour) was developed for the ICARE/CATHARE V2 code version. Currently, the ICARE/CATHARE V2 code allows to:

- simulate the flow pattern in 2D in the whole vessel,
- model the corium behaviour in 2D in the core and in the lower plenum,
- predict the vessel failure,
- provide best-estimate data in order to estimate the FP retention in the upper plenum.

Coupling between ICARE and CATHARE

In ICARE/CATHARE, the ICARE2 part calculates all the phenomena occurring inside the core during the early and late degradation phases, namely thermal-hydraulics (1-D two phase flow in parallel multi-channels, no cross flows), thermal and mechanical behaviour of the fuel and control rods (ballooning, burst, melting, …), chemical interactions (Zr, Fe and B_4C oxidation, UO_2 dissolution, …), fission product release, 2D relocation of materials, debris beds and molten pools formation and behaviour. As for CATHARE2, it calculates the two-phase thermal-hydraulics in the lower and upper plenum and in the rest of the RCS (primary and secondary circuits) with a set of 1D or 0D elements.

The last version of the coupling, ICARE/CATHARE V2, is based on ICARE2 V3mod2.0 and CATHARE2 V2.5_1 (latest CATHARE version released in 2005, which allows a three dimensional description of the whole vessel).

The core (or vessel) geometry to be modelled is defined according to special structural objects which are called “macro-components” in the ICARE2 terminology.

There are several kinds of available macro-components, each one corresponding to an element of the reactor, such as the control rods, the fuel rods, the horizontal plates, the spacer grids, the surrounding walls, the upper and lower heads, the coolant fluid, the flowing corium, etc.

In ICARE/CATHARE V2, the thermal-hydraulics and the degradation can be properly simulated on a 2D meshing covering the whole vessel. Then, a 2-D axial and radial meshing can be defined on these geometrical elements.

[5] P. Chatelard, J. Fleurot, O. Marchand, P. Drai, Assessment of the ICARE/CATHARE V1 severe accident code, ICONE-14 Conference, Miami, Florida, U.S.A, July 17-20, 2006, NURETH-11 Conference, Avignon, France, October 2-6, 2005.

Core degradation: main physical models

Degradation of fuel and control rods

The phenomena taken into account to predict the mechanical behaviour of fuel rods are ballooning, creep (with cladding burst detection) and cladding failure at high temperatures (ZrO_2 shell failure). The physical criteria retained to trigger the cladding failure have been established according to the interpretation of the PHEBUS bundle tests FPT0, FPT1 and FPT2.

The fuel loss of geometry is based on an early fuel liquefaction process as observed in the PHEBUS experiments. To take into account this phenomenon which can take place at a rather low temperature far below the UO_2 melting temperature, the solidus and liquidus temperature of both UO_2 and ZrO_2 materials have been reduced to [2550-2600]K.

A dissolution model assumes a fast interaction between a liquid mixture rich in Zircaloy and both solid UO_2 and ZrO_2, leading to a simultaneous dissolution of both oxides.

An instantaneous dissolution of the Zircaloy guide tube at the time of steel clad melting is assumed. A solid-solid interaction between steel and Zircaloy, in case of contact between the absorber rod cladding and the Zircaloy guide tube, and a possible dissolution of the Zircaloy guide tube by molten AIC (Silver-Indium-Cadmium alloy) are also taken into account.

Oxidation

Standard physical models are used to calculate the oxidation by steam of the main metallic structures (Zircaloy, stainless steel) and boron carbide pellets before their slumping. Moreover, a specific model is devoted to the oxidation by steam of the U-Zr-O relocated mixtures. This recent model allows to take into account the thermal power and the hydrogen production due to the oxidation of materials contained in melted materials. It has an impact on the relocation velocity of such melts (the viscosity varies according to the oxidation degree).

Material relocation

When a structure is molten or dissolved, the resulting liquid mixture may move axially and/or radially on the 2D-meshing, properly accounting for the presence of obstacles such as spacer grids, plates, shrouds and possible local blockages due to refrozen materials.

Lower-head vessel failure

In the V2-2D calculation, several types of possible rupture modes are computed for the lower vessel head (plastic, creep, melting). This rupture cannot be computed in the V2-1D calculation because the lower plenum is a CATHARE volume.

11.3 ATHLET-CD

The system code ATHLET-CD (**A**nalysis of **TH**ermal-hydraulics of **LE**aks and **T**ransients with **C**ore **D**egradation) is designed to describe the reactor coolant system thermal-hydraulic response during severe accidents, including core damage progression as well as fission product and aerosol behaviour, to calculate the source term for containment analyses, and to evaluate accident management measures. It is being developed by GRS in cooperation with the Institut für Kernenergetik und Energiesysteme (IKE), University of Stuttgart. ATHLET-CD includes also the aerosol and fission product transport code

SOPHAEROS which is being developed by the French Institut de Radioprotection et de Sûreté Nucléaire (IRSN).

The ATHLET-CD structure is highly modular in order to include a manifold spectrum of models and to offer an optimum basis for further development. ATHLET-CD contains the original ATHLET models for comprehensive simulation of the thermo-fluid-dynamics in the coolant loops and in the core. The ATHLET code comprises a thermo-fluid-dynamic module, a heat transfer and heat conduction module, a neutron kinetics module, a general control simulation module, and a general-purpose solver of differential equation systems called FEBE. The thermo-fluid-dynamic module is based on a six-equation model, with fully separated balance equations for liquid and vapour, complemented by mass conservation equations for up to 5 different non-condensable gases and by a boron tracking model. Alternatively, a five-equation model, with a mixture momentum equation and a full-range drift-flux formulation for the calculation of the relative velocity between phases is also available. Specific models for pumps, valves, separators, mixture level tracking, critical flow etc. are also included in ATHLET.

The rod module ECORE consists of models for fuel rods, absorber rods (AIC and B_4C) and for the fuel assemblies including BWR-canisters and -absorbers. The module describes the mechanical rod behaviour (ballooning), zirconium and boron carbide oxidation (Arrhenius-type rate equations), Zr-UO_2 dissolution as well as melting of metallic and ceramic components. The melt relocation (candling model) is simulated by rivulets with constant velocity and cross section, starting from the node of rod failure. The model allows oxidation, freezing, re-melting, re-freezing and melt accumulation due to blockage formation. The feedback to the thermal-hydraulics considers steam starvation and blockage formation. Besides the convective heat transfer, energy can also be exchanged by radiation between fuel rods and to surrounding core structures.

The release of fission products is modelled by rate equations or by a diffusion model within the module FIPREM. The release of aerosols is described by rate equations. The release of control rod materials (Ag, In, Cd) is based on temperature functions taking into account the partial pressure of the material gases. The transport and retention of aerosols and fission products in the coolant system are simulated by the code SOPHAEROS.

For the simulation of debris beds a specific model MEWA is under development with its own thermal-hydraulic equation system, coupled to the ATHLET-thermo-fluid-dynamics on the outer boundaries of the debris bed. The transition of the simulation of the core zones from ECORE to MEWA depends on the degree of degradation in the zone. The code development comprises also late phase models for core slumping, melt pool behaviour and vessel failure.

The code system ATHLET/ATHLET-CD is coupled to the containment code system COCOSYS, and it is the main process model within the German nuclear plant analyzer ATLAS. The ATLAS environment allows not only a graphical visualisation of the calculated results but also an interactive control of data processing

The code validation is based on integral tests and separate effect tests, proposed by the CSNI validation matrices, and covers thermal-hydraulics, bundle degradation as well as release and transport of fission products and aerosols. Recent post-test calculations have been performed for the out-of pile bundle experiments QUENCH-07, QUENCH-08, QUENCH-09, QUENCH-10 and QUENCH-11 as well as for the in-pile experiments Phébus FPT2 and FPT3. The TMI-2 accident is used to assess the code for reactor applications.

The development and the validation of ATHLET-CD are sponsored by the German Federal Ministry of Economics and Technology (BMWi).

11.4 FRAPTRAN-GENFLO

FRAPTRAN-GENFLO is a coupled combination of a non-equilibrium thermal hydraulic model and a detailed fuel description.

In the general thermal hydraulic model GENFLO, the liquid and vapour mass, mixture momentum and liquid and vapour energy (enthalpy) conservation equations are solved for a single flow channel applying 5-equation formalism, where the phase separation is solved in a correlation form using the drift flux formulation. The primary integration variables are the local pressure, the mass fluxes of the liquid and vapour phases, and the enthalpies of liquid and vapour. The primary variables may be used for deriving the fluid temperature and void fraction (volumetric vapour content) in the fluid. The fluid temperature and heat transfer coefficient from the heat transfer calculation for each axial level at successive time steps can be supplied as boundary conditions for the fuel code FRAPTRAN.

In parallel, GENFLO integrates its own fuel transient temperature based on the axial power profile. The coupling methodology guarantees the energy conservation and also makes it possible to run GENFLO as a standalone code, if the details of fuel behaviour covered by FRAPTRAN are not particularly desired. In the combined simulation mode, the power history is delivered from FRAPTRAN to GENFLO, and FRAPTRAN receives the surface heat transfer coefficients and the local bulk temperature for the heat transfer calculation and the local pressure that is used in the ballooning calculation.

In a generic LWR application, pressure, temperature and flow boundary conditions are provided by a separate calculation with a system code. These can be used as a boundary condition of the independent FRAPTRAN code as well. At VTT the host code may be RELAP5, APROS or TRAB-3D-SMABRE. For analysing the IFA-650 experiment, GENFLO was extended from its original format, to describe the experimental loop in sufficient detail. Such detail includes the long injection line into the rig and the outflow line through the blow-down valves into the blow-down tank that define the pressure boundary condition. The long external pipelines have a strong contribution to the blow-down characteristics during the first 100 seconds of the experiment.

The phase separation model based on the drift flux model customarily includes two empirical parameters, the average drift flux velocity between phases and a distribution parameter describing the velocity profiling. The coefficients are selected so as to give the best approximation for the bubble flow at low void fractions and vapour droplet flow at high void fractions. The intermediate region exhibits a smooth transition form the low relative velocity zone with bubbles to the high relative velocity zone with droplets.

The non-condensable gas field allows describing the hydrogen released during the cladding oxidation. In LOCA conditions typically the wall is wetted when the temperature is below the Leidenfrost temperature, and dry above it. The heat transfer coefficient for the wetted wall is typically defined via correlations for the convective heat transfer from the wall to the gas, from the wall to the liquid, and for the boiling heat transfer from the wall to the mixture. With sub-cooled liquid, a division of the heat flux into liquid heating and evaporation portions is applied. The heat transfer to the liquid is limited by the critical heat flux correlation. In boiling channels, the main parameter affecting the critical heat flux is the amount coolant, expressed as the void fraction or flow quality. When the void fraction is high enough, the wall heat flux changes into the post-dryout mode, i.e. the surface temperature exceeds the Leidenfrost temperature. In the post-dryout zone, the heat transfer is a combination of inversed annular film boiling, convective heating of steam, and – if the surface temperature is high enough – radiation heat transfer.

Flashing heat transfer is considered as the interfacial heat transfer mode, when the superheated liquid is boiling or the sub-cooled liquid is condensing vapour. In the post-dryout zone, the evaporation of droplets due to superheated vapour is considered as well.

Radiative heat transfer becomes essential at higher temperatures, typically above 600^{o}C. In a full core simulation, the core would be described with axial heat slabs and cylindrically symmetric radial zones and the radial radiation resistivity be defined between the zones. In small-scale applications, the core equals a single fuel rod. The radiation to external structures, like the heater and the vessel wall in the Halden IFA-650 experiments, can be optionally described through view factors.

12. APPENDIX II – BENCHMARK PARTICIPATION

The following table summarizes the participation in the different rounds of calculation.

Round 1: benchmark I – blind calculations, 650.3

Round 2: benchmark I – post-test calculations 1, 650.3

Round 3: benchmark I – post-test calculations 2 (unified boundary conditions)

Round 4: benchmark II – 650.4 / 650.5

Tab. 5 – List of benchmark participants

Organisation	Gesellschaft für Anlagen- und Reaktorsicherheit, Germany (GRS)
Participants	G. Lerchl, K. Trambauer, H. G. Sonnenburg, J. Herb
Code	Athlet-CD
Rounds	1, 2, 3, 4
Organisation	Institut de Radioprotection et de Sûreté Nucléaire (IRSN)
Participants	C. Grandjean
Code	ICARE/CATHARE
Rounds	1, 2, 3, 4
Organisation	Japan Nuclear Energy Safety Organization (JNES)
Participants	T. Nakajima
Code	TRAC-PF1
Rounds	1
Organization	Paul Scherrer Institut (PSI)
Participants	H. Wallin,Y. Aounallah
Code	Falcon, Trace
Rounds	1, 2, 3

Organisation	TÜV NORD EnSys Hannover GmbH & Co.KG
Participants	G. Spykman
Code	Transuranus
Rounds	1, 2, 3
Organization	VTT-Processes
Participants	J.-O. Stengård, S. Kelppe
Code	GENFRA, Fraptran
Rounds	1, 3, 4
Organisation	CEA France
Participants	C. Struzik
Code	Meteor
Rounds	3, 4

13. APPENDIX III – DESCRIPTION OF THE TEST CASES

A comprehensive description of the benchmarks was compiled in modelling packages and sent to the participants on CDs. Experimental results were included for Benchmark II, while for Benchmark I no such data were available at the start of the benchmarking.

13.1 Common features

13.1.1 Loop and blow-down system

The heavy water loop schematically shown in Fig. 39 was used in all experiments. Also the rig and flask were practically identical. The modelling package contains the exact dimensions of the pipes and their elevation.

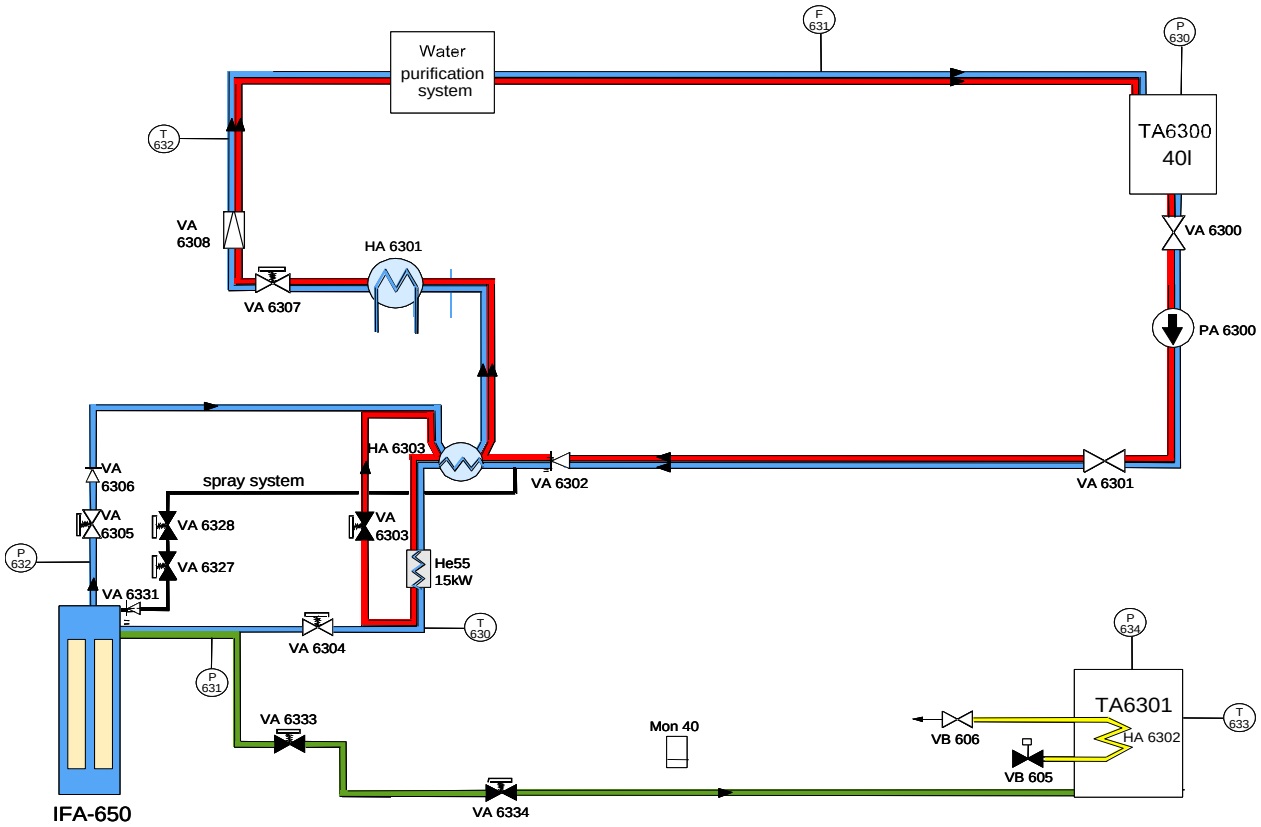

Fig. 39 - Simplified drawing of the loop used for IFA-650 experiments

Blue = flow during forced circulation // **Red** = flow in the isolated loop during natural circulation phase and blow-down of the rig // **Green** = flow from the rig to TA6301 during blow-down

Loop conditions

fluid:	heavy water
pressure:	started with 70 bar
temperature:	started with 235°C
blow-down tank pressure:	2-3 bar (total volume = 100 l, water level before blow-down ~15-20 l)
conditions outside of flask:	standard Halden reactor conditions, coolant is heavy water, temperature is about 235°C and pressure 34 bar

13.1.2 Axial power distribution

Participants were asked to assume an axial power distribution according to the neutron flux distribution measured in the commissioning runs. The profile is shown in Fig. 40.

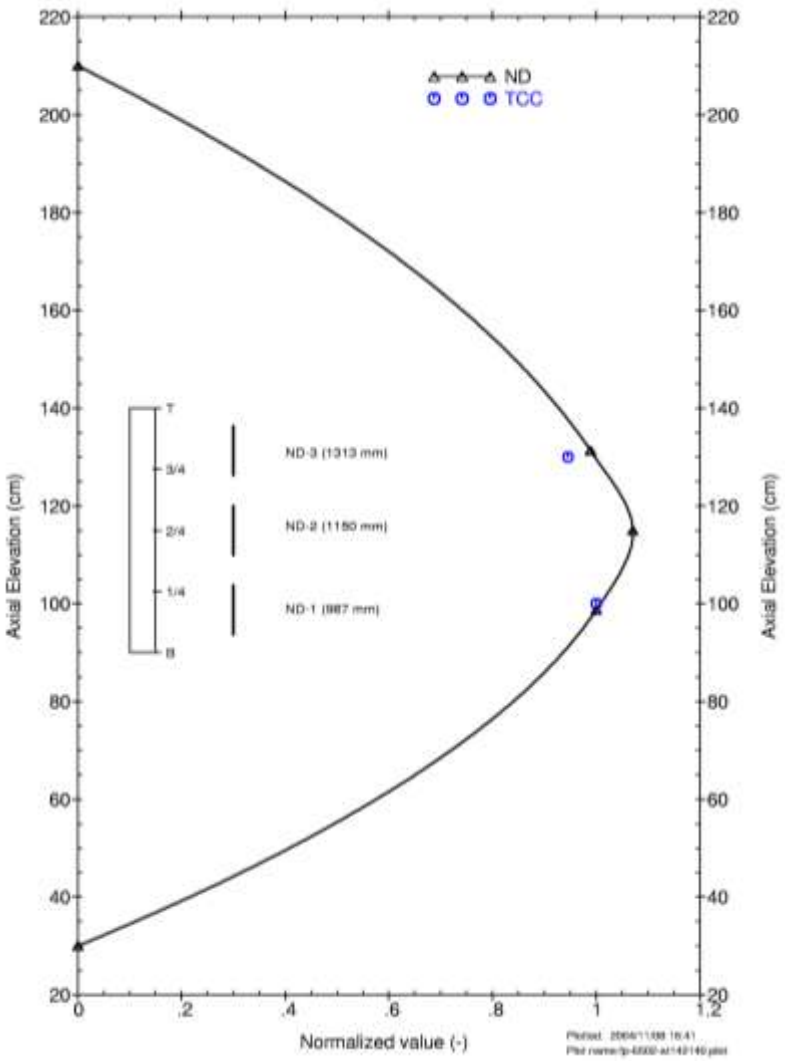

Fig. 40 – Axial power profile in IFA 650.2

13.2 Flask and rig

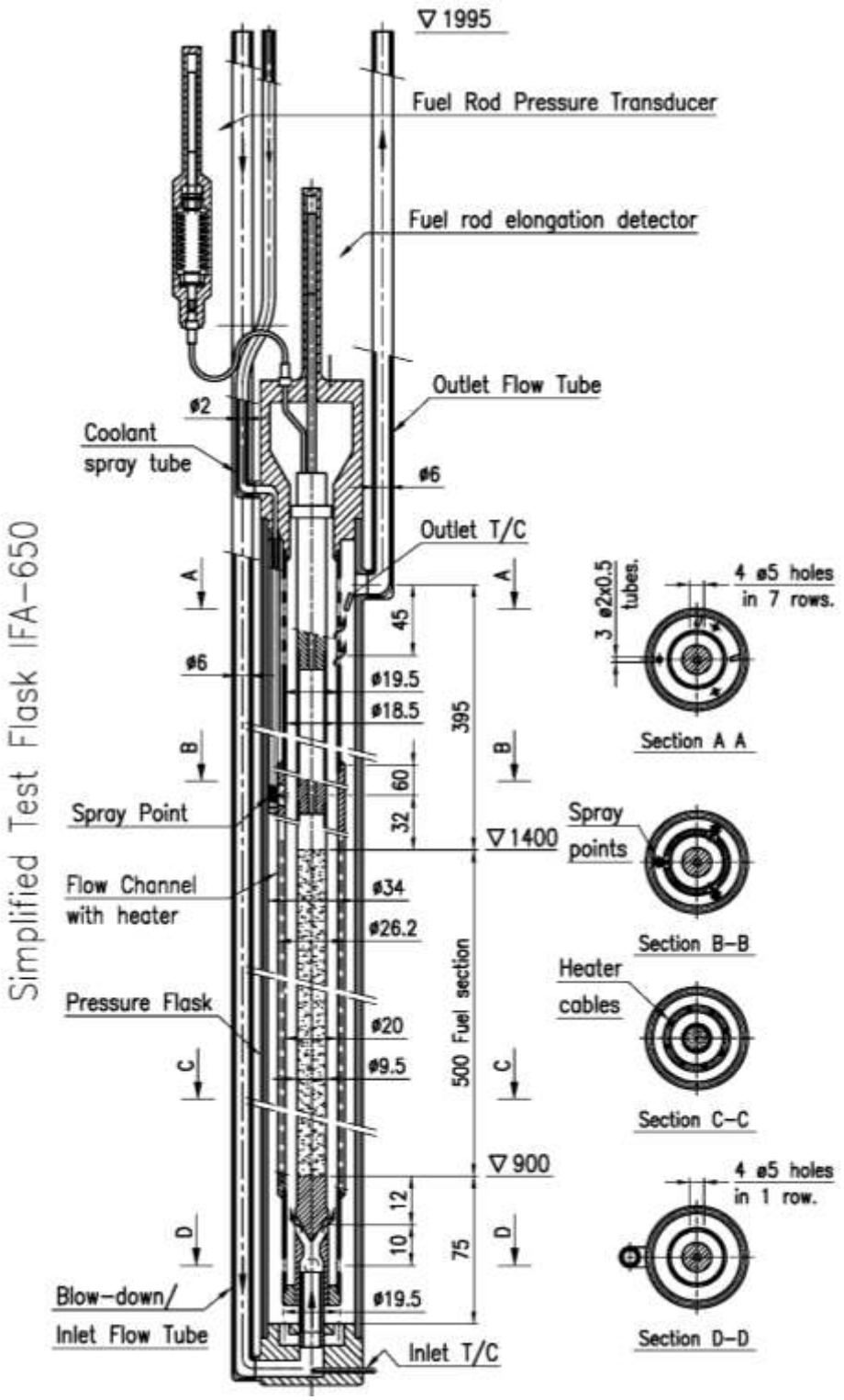

Fig. 41 – Simplified IFA 650 flask

13.3 IFA-650.3

The test had not been executed at the time of starting the benchmark, and consequently not all operation conditions were known. The following specifications for IFA 650.3 were given in the package:

Tab. 6 - Fuel data of IFA-650.3

Items	**Value**
Rod identification	V1-515 / 3
Span between spacer	2-3
Initial enrichment [wt%U_{235}]	3.5
UO_2 density [g/cm^3]	10.39
Cycles	6
Burnup [MWd/kgU]	82
Oxide thickness, mean / max [μm]	25 - 27
Hydrogen content, ppm	250
Length fuel / cladding [mm]	480 / 499.8
Cladding	
- type	DX ELS0.8b
- OD [mm]	10.75
- thickness [mm]	0.725
- liner [mm]	0.150
- chem. comp. of cladding base material	Zry-4, 1.47% Sn
- chem. comp. of the liner	0.84 % Sn, 0.29 % Fe, 0.17 % Cr
Heat treatment	SRA

When prepared for the test, the fuel rod was emptied of fission gases and re-pressurized with Argon at 40 bar (at 25 ºC).

The target cladding temperature for the test was 800 ºC (average of measuring points located 100 mm from both ends of the fuel rod). The temperature was to be maintained for 5-6 minutes.

Tab. 7 - Initial power conditions of the fuel rod and heater:

axial power profile of the fuel rod:	similar to IFA-650.2, see Fig. 40
radial power profile of the fuel rod:	flat
axial power profile of the heater:	flat

Since the target PCT depends on the energy release from the fuel rod and the heater, both only estimated before the actual test execution, participants were asked to apply the following combinations in the calculations:

Tab. 8 – Combinations of fuel and heater power

	Average LHR of the fuel rod	**Heater power**
Case 1	12 W/cm	6 W/cm
Case 2	5 W/cm	15 W/cm
Case 3	8 W/cm	15 W/cm
Case 4	11 W/cm	15 W/cm

13.4 IFA-650.4

The operation conditions were known at the start of the benchmark and included in the data package as measured. The following specifications apply to IFA 650.4:

Tab. 9 - Fuel data of IFA-650.4

Items	**Value**
Rod identification	14D/7
Span between spacer	5-6
Initial enrichment [wt%U_{235}]	3.5
UO_2 density [g/cm^3]	10.39
Cycles	7
Burnup [MWd/kgU]	92
Oxide thickness, mean / max [μm]	10 - 11
Hydrogen content, ppm	50
Length fuel / cladding [mm]	480 / 496.5
Cladding	
- type	DX Zr2.5Nb
- OD [mm]	10.75
- thickness [mm]	0.725
- liner [mm]	0.100
- chem. comp. of cladding base material	Zry-4, Sn 1.53% Fe 0.22% Cr 0.11 % O 0.14 %
- chem. comp. of the liner	O 0.12 %, Nb 2.6 %
Heat treatment	SRA

When prepared for the test, the fuel rod was emptied of fission gases and re-pressurized with Argon at 40 bar (at 25 ºC).

The target cladding temperature for the test was 800 ºC.

13.5 IFA-650.5

The operation conditions were known at the start of the benchmark and included in the data package as measured. The following specifications apply to IFA 650.5:

Tab. 10 - Fuel data of IFA-650.5

Items	**Value**
Rod identification	V1-515 / 7
Span between spacer	5-6
Initial enrichment [wt%U_{235}]	3.5
UO_2 density [g/cm^3]	10.39
Cycles	6
Burnup [MWd/kgU]	83
Oxide thickness, mean / max [μm]	65 - 80
Hydrogen content, ppm	650
Length fuel / cladding [mm]	480 / 500.0
Cladding	
- type	DX ELS0.8b
- OD [mm]	10.75
- thickness [mm]	0.725
- liner [mm]	0.150
- chem. comp. of cladding base material	Zry-4, Sn 1.48 % Fe 0.23 % Cr 0.12 % O 0.14 %
- chem. comp. of the liner	0.84 % Sn, 0.29 % Fe, 0.17 % Cr
Heat treatment	SRA

When prepared for the test, the fuel rod was emptied of fission gases and re-pressurized with Argon at 40 bar (at 25 ºC).

The target cladding temperature for the test was 1100 ºC.

Severe contamination of the system by small fuel particles blown out of the rod into the system tubes was observed as a consequence of IFE-650.4. In order to mitigate this effect, a filter was installed in the blow-down line. This change influenced the dynamics of the system.